Published Online First: November, 2024
https://doi.org/10.21123/bsj.2024.11370
P-ISSN: 2078-8665 - E-ISSN: 2411-7986
Baghdad Science Journal

Stability Analysis of Excessive Carbon Dioxide Gas Emission Model through Following Reforestation Policy in Low-Density Forest Biomass

Furqan Nezar [1], ***Shireen Jawad*** [1], ***Matthias Winter*** [2], ***Anwar Zeb**** [3]

[1] Department of Mathematics, College of Science, University of Baghdad, Baghdad, Iraq.
[2] Department of Mathematics, Brunel University London, Uxbridge UB8 3PH, UK.
[3] Department of Mathematics, COMSATS University Islamabad, Abbottabad Campus, Pakistan.
*Corresponding Author.

Received 15/04/2024, Revised 06/07/2024, Accepted 08/07/2024, Published Online First 20/11/2024

Abstract

Carbon dioxide is the main greenhouse gas contributing to global warming risk. Forest biomass is crucial for the sequestration of atmospheric carbon dioxide; however, the rate of decline in worldwide forest biomass is concerning and can be attributed to anthropogenic activities. Reforestation is essential in this situation to decrease the amount of CO_2 in the atmosphere. Efforts at reforestation can be evaluated according to the financial investment required for their execution. This work presents a nonlinear mathematical model that examines the impact of reforestation and the implementation of reforestation initiatives on regulating atmospheric CO_2 levels. The critical values of the model and their stability are found analytically. The occurrence of transcritical bifurcation around the possible critical points is performed using the Sotomayor theorem. Based on the numerical simulations, the model in the absence of reforestation would put some aspects at risk of extinction. Further, the level of CO_2 in the atmosphere would decrease due to reforestation. Moreover, the numerical analysis indicates that the system experiences a loss of stability without reforestation activities. The system maintains oscillation through Hopf-bifurcation while engaging in reforestation activities.

Keywords: Bifurcation Analysis, Carbon Dioxide Gas Emission Model, Numerical Solutions, Reforestation, Stability Analysis.

Introduction

The world faces several environmental issues. Global warming is among the most dangerous concerns. The fundamental factor that contributes to the danger of global warming is the increased concentration of carbon dioxide CO_2 in the atmosphere [1-3]. The world faces several environmental issues. Overexploitation of our planet has led to global warming, which is responsible for most of these issues. The fundamental factor that contributes to the danger of global warming is the increased concentration of carbon dioxide CO_2 in the atmosphere, leading to natural calamities such as aridity, flooding, desertification, etc. [4]. Human activities, including agriculture, industrialization, urbanization, deforestation, transportation, mining, and energy generation, significantly increase greenhouse gas emissions, particularly carbon dioxide. Climate change is destroying almost every

Published Online First: November, 2024
https://doi.org/10.21123/bsj.2024.11370
P-ISSN: 2078-8665 - E-ISSN: 2411-7986
Baghdad Science Journal

country [5]. Climate change concerns are developing due to rising global temperatures. This is due mainly to high greenhouse gas emissions and accumulation. Human actions have caused global warming, climate change, and negative repercussions on our quality of life [6,7]. These occurrences result in a significant number of fatalities due to physical injuries, inadequate nutrition, and heightened susceptibility to contagious illnesses within the community [8]. Climate changes also impact the occurrence of vector-borne diseases due to the rise in population and the spread of vectors that transmit the disease [9]. Climate changes are estimated to account for 3% of in 2004, 3% of global deaths were attributed to diarrhea, malaria accounted for 3%, and dengue fever accounted for 3.8% of deaths. Heart and breathing problems can get worse during heat waves. Increasing the level of carbon dioxide, CO_2 is primarily responsible for climate change, so it is crucial to produce measures to decrease and stabilize future CO_2 concentrations. For this, it is required to have a deeper comprehension of the main processes that contribute to the rise of CO_2 in atmospheric levels and how they impact the behavior of atmospheric CO_2 [10-12].

Both the numbers of forest biomass and human population have a significant impact on the atmospheric CO_2 level. The increase observed in atmospheric CO_2 concentration can be mainly affected by human activity, specifically the combustion of fossil fuels and changes in land use such as deforestation. The burning of fossil fuels is thought to be responsible for around two-thirds of the increase in atmospheric CO_2, with land use changes accounting for the remaining fraction. Nevertheless, managing the amount of CO_2 in the atmosphere depends on forest biomass. Through photosynthesis, forests absorb gigatons of CO_2, which helps lower global CO_2 levels in the atmosphere. Forest biomass is essential to the dynamics of atmosphericCO_2. Furthermore, one of the main causes of the increased CO2 levels in the atmosphere is the natural CO_2 absorber's depletion as a result of human activity. Hence, realizing the chemistry between human population, forest biomass, and carbon dioxide yields enhanced understanding for forecasting and managing future levels of atmospheric CO_2 [13-15]. Some mathematical models have been presented to analyze the impact of different causes on atmospheric CO_2 concentration [16-18]. For instance, Tennakone [13] has discussed the relationship between biomass and carbon dioxide by applying a mathematical model. This study highlights that wide-ranging deforestation messes up biomass and carbon dioxide equilibrium. A feedback model [14] has been employed to investigate the correlation between global warming and human activities. This study demonstrates that human activities contribute to the generation of CO_2, which in turn has a destabilizing impact. Caetano et al. [8] have established a connection between the atmospheric concentration of CO_2 and variables such as forest area and gross domestic product. The researchers have included reforestation and clean technology as control variables in their study to manage atmospheric CO_2 levels. They have optimized the overall expenditure in reforestation and clean technology to achieve the target level of CO_2 [19-21].

Researchers usually utilize the Allee effect to describe a phenomenon where a population experiences a decrease in its growth rate per individual when the population density or size decreases[22-24]. Based on the available literature, there is currently no mathematical model that investigates the intricate relationship between atmospheric CO_2, human population, and low-density forest biomass. Hence, it has been developed a mathematical model in the current study to investigate the influence of reforestation policy in low-density forests on the dynamics of excessive carbon dioxide gas emission model by incorporating the weak Allee effect in the forest's biomass growth.

The current paper is structured in the following manner: In the following section, it has been established a mathematical model that governs the dynamics of the problem. The model's stability analysis is described in Section 3. In Section 4, the criterion for the presence of bifurcation by selecting an appropriate bifurcating parameter is established. Numerical simulation is performed in Section 5 to validate the analytical results, and the study is ultimately concluded in Section 6.

Published Online First: November, 2024
https://doi.org/10.21123/bsj.2024.11370
P-ISSN: 2078-8665 - E-ISSN: 2411-7986
Baghdad Science Journal

Model Formulation

This section presents a mathematical model that aims to understand how the lack of forest biomass and the following reforestation policy influence the dynamics of carbon dioxide gas. The model considers dynamical variables. The carbon dioxide concentration that is excessive in the atmosphere $c(t)$, the forest biomass $p_1(t)$, the reforestation of forest efforts $p_2(t)$, the human population density $p_3(t)$.

The model was created based on the following assumptions:

1. The present state of climate change is primarily due to the excessive release and buildup of the greenhouse gas carbon dioxide into the atmosphere[14].
2. Human activities, such as the burning of fossil fuels at excessive rates, the fast expansion of industry, the construction of cities, the clearing of forests, and contemporary lifestyles, are significant contributors to the ever-increasing atmospheric concentration of carbon dioxide and reduce green spaces.it is postulated that the human population consistently exploits forest biomass to sustain itself. As a result of population growth, forest areas are removed for agricultural and infrastructure development, which reduces the forest biomass's carrying capacity[14].
3. The growth of the forest biomass density follows a weak Allee effect growth pattern[24-26].
4. It is postulated that the increased mortality rate of the human population is a consequence of the detrimental impacts of carbon dioxide[21].
5. Raising awareness of the risks of high carbon dioxide levels, preventing deforestation, and promoting conservation legislation can reduce emissions into the atmosphere[4].
6. As forests absorb carbon dioxide from the atmosphere through the process of photosynthesis, it can be hypothesized that a reduction in CO_2 concentration occurs as a result of forest biomass[8].
7. Reforestation initiatives are applied to raise forest biomass. Also, it has been assumed that some of the reforestation efforts shrink due to their inefficacy or some financial obstacles[19].

Under the above assumptions, the following set of ordinary differential equations is obtained:

$$\frac{dc}{dt} = r_1 + e_1 p_1 + e_2 p_3 - e_3 c p_1 - \mu_0 c - \mu_1 c = f_1(c, p_1, p_3)$$

$$\frac{dp_1}{dt} = r_2 p_1 \left(1 - \frac{p_1}{m_1}\right)\left(\frac{p_1}{e_4 + p_1}\right) + e_5 p_1 p_2 - e_6 p_1 p_3 - \mu_2 p_1 = f_2(p_1, p_2, p_3) \qquad 1$$

$$\frac{dp_2}{dt} = r_3 (m_1 - p_1) - \mu_3 p_2 = f_3(p_1, p_2)$$

$$\frac{dp_3}{dt} = r_4 p_3 \left(1 - \frac{p_3}{m_2}\right) - e_7 c p_3 + e_8 p_1 p_3 = f_4(c, p_1, p_3)$$

with the initial conditions $c^0 \geq 0, p_1^0 \geq 0, p_2^0 \geq 0$ and $p_3^0 \geq 0$. Due to the biological nature of the system, all parameters and variables in the model are non-negative and are clearly described in Table 1.

Table 1. Explanation of system's (1) parameters.

Parameter	Explanation
r_1	CO_2 emission rate from natural sources.
r_2	Intrinsic growth rate of the forest biomass.
r_3	Coefficient of implementation rate for reforestation initiatives.
r_4	Intrinsic growth rate of the human population.
e_1	Coefficient of CO_2 emission from forest sources.
e_2	Coefficient of CO_2 emission from anthropogenic sources.
e_3	Coefficient of CO_2 uptake by forest biomass as a result of photosynthesis.
e_4	Allee threshold.
e_5	Reforestation-induced Forest biomass growth coefficient.
e_6	Rate of deforestation.
e_7	The human population decline rate coefficient attributable to CO_2.
e_8	Human population expansion resulting from forest biomass.
m_1	Carrying capacity for the forest biomass.
m_2	Carrying capacity for the human population.
μ_0	Natural CO_2 depletion due to good conservation strategies.
μ_1	Coefficient of natural depletion of atmospheric CO2.
μ_2	Coefficient of natural depletion of forest biomass.
μ_3	Coefficient of decline in reforestation initiatives.

Further, Fig 1 illustrates the schematic sketch of the system (1) under examination.

Published Online First: November, 2024
https://doi.org/10.21123/bsj.2024.11370
P-ISSN: 2078-8665 - E-ISSN: 2411-7986
Baghdad Science Journal

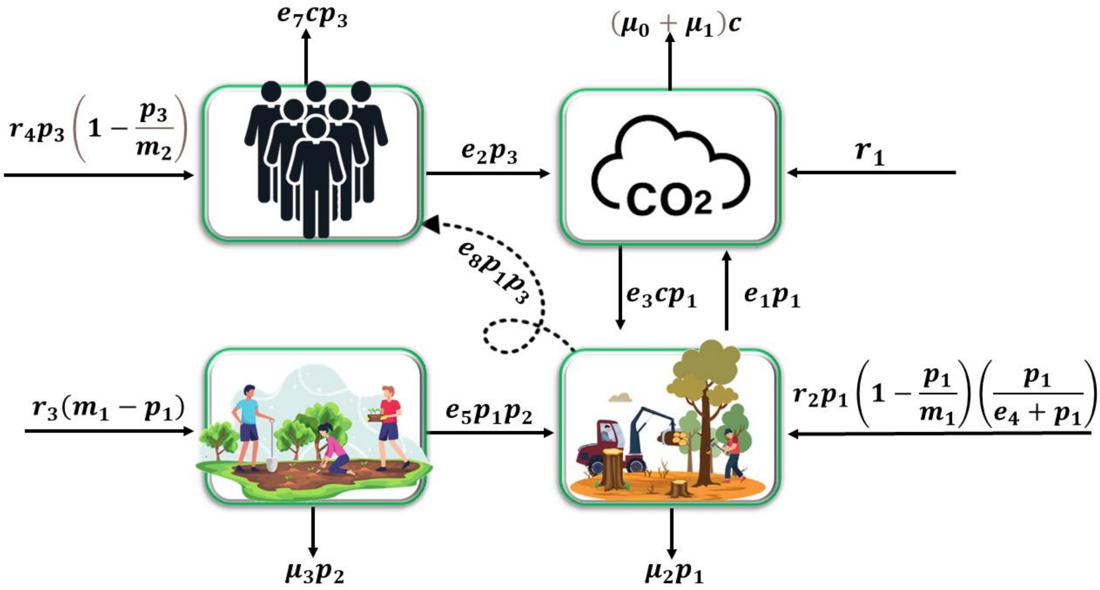

Figure 1.The schematic sketch of system (1).

Theorem 1: All system's (1) solutions $c(t), p_1(t), p_2(t)$ and $p_3(t)$ that start with positive initial conditions c^0, p_1^0, p_2^0, p_3^0 are also positive.

Proof: By integrating the right-hand functions of the model (1) for $c(t), p_1(t), p_2(t)$ and $p_3(t)$, the following is obtained

$$c(t) \geq c^0 exp\left\{\int_0^t\left[-\left(e_3\left(\ p_1^0\ exp\left\{\int_0^t[r_2(1-\frac{p_1(\tau)}{m_1}\right)\left(\frac{p_1}{e_4+p_1}\right)+e_5p_2(\tau)-e_6p_3(\tau)-\mu_2\right]d\tau\right)+\mu_1+\mu_0\right]d\tau\right\}.$$

$$p_1(t)=p_1^0 exp\left\{\int_0^t\left[r_2\left(1-\frac{p_1(\tau)}{m_1}\right)\left(\frac{p_1(\tau)}{e_4+p_1(\tau)}\right)+e_5p_2(\tau)-e_6p_3(\tau)-\mu_2\right]d\tau\right\}.$$

$$p_2(t) \geq p_2^0\ exp[-\mu_2 t].$$

$$p_3(t)=p_3^0 exp\left\{\int_0^t\left[r_4\left(1-\frac{p_3(\tau)}{m_2}\right)-e_7c(\tau)+e_8p_1(\tau)\right]d\tau\right\}.$$

Then $c(t)\geq 0, p_1(t)\geq 0, p_2(t)\geq 0$ and $p_3(t)\geq 0$ for all $t>0$. Therefore, the interior of R_+^4 is an invariant set.

To find the attractive region of the system (1), it may use the following lemma in this setting:

Lemma 1: (Comparison lemma) Assume that $u, v > 0$ with $w(0)>0$. Then for $\frac{dw}{dt}\leq(u-vw(t))$, $\text{Lim}_{\sup_{t\to\infty}} w(t)\leq\frac{u}{v}$ and also for $\frac{dw}{dt}\geq(u-vw(t))$, $\lim\inf_{t\to\infty} w(t)\geq\frac{u}{v}$.

Theorem 2: The set $\omega=\{(c,p_1,p_2,p_3)\in R_+^4: 0\leq c\leq c_m;\ 0\leq p_1\leq m_1;\ 0\leq p_2\leq p_{2m};\ 0\leq p_3\leq p_{3m}\}$ attracts all the solutions $c(t), p_1(t), p_2(t)$ and $p_3(t)$ initiating in R_+^4.

Proof: From the second equation of system (1), the following is obtained

$$\frac{dp_1}{dt}=r_2p_1\left(1-\frac{p_1}{m_1}\right)\left(\frac{p_1}{e_4+p_1}\right)+e_5p_1p_2-e_6p_1p_3-\mu_2p_1\leq r_2p_1\left(1-\frac{p_1}{m_1}\right).$$

Thus, for $t\to\infty$ then $p_1(t)\leq m_1$. From the third equ,

$$\frac{dp_2}{dt}=r_3(m_1-p_1)-\mu_3p_2\leq r_3m_1-\mu_3p_2.$$

Then, applying the Comparison Lemma yield:

$$\text{Lim}_{\sup_{t\to\infty}} p_2(t)\leq\frac{r_3m_1}{\mu_3}=p_{2m}.$$

Using the same technique, it yields

$$\text{Lim}_{\sup_{t\to\infty}} p_3(t)\leq\frac{(r_4+e_8m_1)m_2}{r_4}=p_{3m}.$$

Published Online First: November, 2024
https://doi.org/10.21123/bsj.2024.11370
P-ISSN: 2078-8665 - E-ISSN: 2411-7986
Baghdad Science Journal

$\text{Lim}_{\sup_{t\to\infty}} c(t) \le \frac{r_1 r_3 + e_1 m_1 r_3 + (r_3 + e_8 m_1) e_2 m_2}{r_3(\mu_0 + \mu_1)} = c_m.$

Thus, all system (1) solutions that are initiated in R_+^4 are attracted to the region

$\omega = \{(c, p_1, p_2, p_3) \in R_+^4 : 0 \le c \le c_m;\ 0 \le p_1 \le m_1;\ 0 \le p_2 \le p_{2m};\ 0 \le p_3 \le p_{3m}\}.$

Existence of equilibria

System (1) has six non-negative equilibrium points, namely:

1. The carbon dioxide gas equilibrium point $E_1 = (\tilde{c}, 0,0,0)$. The given equilibrium represents a scenario in which the system is devoid of both human population and forestry biomass, and the atmospheric concentration of carbon dioxide gas is $\tilde{c} = \frac{r_1}{\mu_0 + \mu_1}$.
2. The carbon dioxide gas-human equilibrium point$E_2 = (\hat{c}, 0,0, \hat{p}_3)$, where the human population is $\hat{p}_3 = \frac{m_2(r_3(\mu_0+\mu_1) - e_7 r_1)}{r_4(\mu_0+\mu_1) - m_2 e_2 e_7}$ and carbon dioxide gas is $\hat{c} = r_1 + \frac{e_2 \hat{p}_3}{\mu_0 + \mu_1}$. E_2 is feasible, provided that one of the following conditions holds

$$\left.\begin{array}{l} \left(\frac{r_4(\mu_0+\mu_1)}{e_7}\right) > max\{r_1, m_2 e_2\}, \\ \left(\frac{r_4(\mu_0+\mu_1)}{e_7}\right) < min\{r_1, m_2 e_2\}. \end{array}\right\} \quad 2$$

3. The carbon dioxide gas-forest equilibrium point $E_3 = (\check{c}, \check{p}_1, 0,0)$, where the carbon dioxide gas is $\check{c} = \frac{(r_1 + e_1 p_1)}{e_3 p_1 + \mu_0 + \mu_1}$ and the forestry biomass $\check{p}_1$ is the positive root of the following equation

$$g(p_1) = r_2 {p_1}^2 - (r_2 m_2 - \mu_2 m_1) p_1 + \mu_2 m_1 e_4.$$

Clearly, $g(m_1) = m_1[(r_2 + \mu_2) m_1 + e_4 \mu_2 - r_2 m_2)]$, $g(0) = \mu_2 m_1 e_4 > 0$ and $g'(p_1) = 2 r_2 p_1 + \mu_2 m_1 - r_2 m_2$. Therefore, $g(p_1) = 0$ has a unique positive root, say $\check{p}_1$ in the interval $(0, m_1)$ if $g(m_1) < 0$ and $g'(p_1) < 0$, that means if

$$r_2 m_2 > max\{(r_2 + \mu_2) m_1 + e_4 \mu_2, 2 r_2 p_1 + \mu_2 m_1\} \quad 3$$

4. The forest-free equilibrium point $E_4 = (\bar{c}, 0, \bar{p}_2, \bar{p}_3)$, where, $\bar{c} = \frac{(r_1 + e_1 \bar{p}_3)}{\mu_0 + \mu_1}$, $\bar{p}_2 = \frac{r_3 m_1}{\mu_3}$ and $\bar{p}_3 = \frac{(r_3 m_2[\mu_0+\mu_1] - r_1 m_2 e_7)}{r_3[\mu_0+\mu_1] + m_2 e_7 e_2}$. For $\bar{p}_3$ to be positive, the following would be the case:

$$r_3[\mu_0 + \mu_1] > e_7 r_1 \quad 4$$

5. The reforestation-free equilibrium point $E_5(\ddot{c}, \ddot{p}_1, 0, \ddot{p}_3)$, where, $\ddot{c} = \frac{r_1 + e_1 \ddot{p}_1 + e_2 \ddot{p}_3}{e_3 \ddot{p}_1 + \mu_0 + \mu_1}$, $\ddot{p}_3 = \frac{r_4 m_2 (e_3 \ddot{p}_1 + \mu_0 + \mu_1 - e_7) + \ddot{p}_1 m_2(-e_7 e_1 + e_8(\ddot{p}_1 e_3 + \mu_0 + \mu_1)}{r_4(e_3 \ddot{p}_1 + \mu_0 + \mu_1) - e_2 e_7 m_2}$, and $\ddot{p}_1$is the root of the following equation

$$A_0 \ddot{p}_1^3 + A_1 \ddot{p}_1^2 + A_2 \ddot{p}_1 + A_3 = 0, \quad 5$$

Where, $A_0 = e_3(m_1 m_2 e_6 e_8 - r_4 r_2)$.

$$A_1 = r_2 r_4(e_3 - \mu_0 - \mu_1) + m_1 m_2 e_6 e_8(\mu_0 + e_3 - e_3 e_4) + m_1 e_6(r_4 m_2 e_5 + m_2 e_7 + m_1 \mu_1 e_8) + m_2 r_2 e_2 e_7 + m_1 \mu_2 r_4 e_3.$$

$$A_2 = m_1[r_2 r_4(\mu_0 + \mu_1) - m_2 e_6(e_1 e_4 e_7 - r_4 e_4 e_5 + \mu_0 e_4 e_8 + \mu_0 r_4 + \mu_1 r_4 - r_2 e_7) - \mu_2(r_3 e_3 e_4 - \mu_0 r_4 - \mu_1 r_4 + m_2 e_2 e_7) + m_1 \mu_1 e_4 e_6 e_8 - r_2 m_2 e_2 e_7].$$

$$A_3 = m_1 e_4[m_2 e_7(r_1 e_6 + \mu_2 e_2) - r_4 m_2 e_6(\mu_0 + \mu_1) - \mu_2 r_4(\mu_0 + \mu_1).$$

Using Descartes's rule of sign[27-29], Eq 5 has a unique positive root, say $p_1 = \hat{p}_1$, if one of the following sets conditions hold:

$A_0 > 0$ and $A_i < 0, i = 2,3,$

$A_i > 0, i = 0,1$ and $A_3 < 0,$

$A_5 < 0$ and $A_i > 0, i = 2,3,$

$A_i < 0, i = 0,1$ and $A_3 > 0.$

Published Online First: November, 2024
https://doi.org/10.21123/bsj.2024.11370
P-ISSN: 2078-8665 - E-ISSN: 2411-7986
Baghdad Science Journal

Clearly, $\hat{p}_3 > 0$ if one of the following conditions holds:

$$\left(\frac{e_3\ddot{p}_1 + \mu_0 + \mu_1}{e_7}\right) > max\left\{\frac{r_4 + \ddot{p}_1 e_1}{r_4 + \ddot{p}_1 e_8}, \frac{e_2 m_2}{r_4}\right\}$$

$$\left(\frac{e_3\ddot{p}_1 + \mu_0 + \mu_1}{e_7}\right) < min\left\{\frac{r_4 + \ddot{p}_1 e_1}{r_4 + \ddot{p}_1 e_8}, \frac{e_2 m_2}{r_4}\right\}$$

6. The reforestation equilibrium point $E_6 = (c^*, p^*{}_1, p^*{}_2, p^*{}_3)$, where, $c^* = \frac{r_1 + e_1 p_1^* + e_2 p_3^*}{e_3 p_1^* + \mu_1 + \mu_0}$, $p_2^* = \frac{r_3(m_1 - p_1^*)}{\mu_3}$, $p_3^* = \frac{m_2(r_3 - e_7 c^* + e_8 p_1^*)}{r_3}$ and p_1^* is the positive root of the following equation

$$B_0 p_1^{*3} + B_1 p_1^{*2} + B_2 p_1^* + B_3 = 0 \qquad 6$$

Where, $B_0 = -\mu_3 e_3 (r_2 r_4 + m_1 m_2 e_6 e_8) - m_1 r_3 r_4 e_3 e_5. < 0$,

$$B_1 = \mu_3[m_1(r_2 r_4 e_3 - m_2 e_1 e_6 e_7 - \mu_2 e_3 e_4 - m_2 r_3 e_3 e_6 - \mu_2 e_3 - \mu_0 m_2 e_6 e_8 - m_2^2 e_2 e_6 e_7 e_8 - m_2 e_3 e_4 e_6 e_8) - r_2(\mu_0 r_4 - \mu_1 r_4) - \mu_1 m_2 e_6 e_8] + r_3 e_5 m_1 (r_4 m_1 e_3 - r_4 e_3 e_4 - \mu_0 - e_2 e_7).$$

$$B_2 = m_1[\mu_3(r_2(\mu_0 r_4 + \mu_1 r_4 + \mu_2 e_2 e_7) - e_7(m_2 e_1 e_4 e_6 - m_1 e_2 e_5 r_3 - m_2 r_1 e_6 - m_2 e_1 e_4 e_6 e_7 r_1 - m_2^2 e_2 e_3 e_6 e_8 - \mu_2 m_2 e_2) - \mu_2(\mu_0 + \mu_1) - m_2 r_3 e_6(\mu_0 + \mu_1 + m_2 e_2) - \mu_0 m_2 e_4 e_6 e_8) + r_3 e_5(m_1 r_4 e_3 e_4 + r_4 e_4 m_1 \mu_0 + m_1 e_2 e_7 - e_4 e_2 e_7 - m_1 \mu_0 r_4 - m_2 e_2 e_4 e_7)].$$

$B_3 = m_1^2 r_3 r_4 e_4 e_5(\mu_0 + \mu_1) + m_1 e_4[(m_1 m_2 r_3 e_2 e_5 e_7 + \mu_3 m_2 r_1 e_6 e_7 - m_2 \mu_3 r_4 e_6(\mu_0 + \mu_1) - \mu_2 \mu_3 (r_4(\mu_0 + \mu_1) + e_2 e_7)]$.

Using Descartes's rule of sign, Eq 6 has a unique positive root, say $p_1 = p_1^*$ if one of the following sets of conditions holds:

$$B_i, i = 2,3 > 0,$$

$$B_1 < 0 \text{ and } B_3 > 0.$$

Further, $p_3^* > 0$ if one of the following conditions holds:

$$r_3 + e_8 p_1^* > e_7 c^*$$

Stability Analysis

This section explores the local stability behavior of the system's (1) equilibrium points. The Jacobin matrix at any point, say (c, p_1, p_2, p_3), can be written as:

$$J(c, p_1, p_2, p_3) = \begin{bmatrix} -e_3 p_1 - \mu_0 - \mu_1 & e_1 - e_3 c & 0 & e_2 \\ 0 & a_{22} & e_5 p_1 & -e_6 p_1 \\ 0 & -r_3 & -\mu_3 & 0 \\ -e_7 p_3 & e_8 p_3 & 0 & r_4 - \frac{2 r_4 p_3}{m_2} - e_7 c + e_8 p_1 \end{bmatrix},$$

where $a_{22} = \frac{r_2 p_1[2m_1(e_4 + p_1) - p_1(2p_1 + 3e_4)]}{m_1(e_4 + p_1)^2} + e_5 p_2 - e_6 p_3 - \mu_2$. Consequently, the following is obtained.

1. The Jacobian matrix at $E_1 = (\tilde{c}, 0,0,0)$ is given as:

$$J(E_1) = \begin{bmatrix} -(\mu_0 + \mu_1) & e_1 - \left(\frac{e_3 r_1}{\mu_0 + \mu_1}\right) & 0 & e_2 \\ 0 & -\mu_2 & 0 & 0 \\ 0 & -r_3 & -\mu_3 & 0 \\ 0 & 0 & 0 & r_4 - \left(\frac{e_7 r_1}{\mu_0 + \mu_1}\right) \end{bmatrix},$$

Then, $J(E_1)$ has the eigenvalues $\lambda_{11} = -(\mu_0 + \mu_1) < 0$, $\lambda_{12} = -\mu_2 < 0$, $\lambda_{13} = -\mu_3 < 0$, $\lambda_{14} =$

Published Online First: November, 2024
https://doi.org/10.21123/bsj.2024.11370
P-ISSN: 2078-8665 - E-ISSN: 2411-7986
Baghdad Science Journal

$r_4 - \left(\frac{e_7 r_1}{\mu_0+\mu_1}\right)$. Then E_1 is a locally asymptotic stable if

$$r_1 > \frac{r_4(\mu_0+\mu_1)}{e_7}. \quad 7$$

This condition states that in the absence of human population and forest biomass, the carbon dioxide gas point will be stable only if its natural growth rate (nonanthropogenic) is greater than the intrinsic growth rate of the human population. Moreover, E_1 has a locally unstable manifold in the P_3-direction provided $r_1 < \frac{r_4(\mu_0+\mu_1)}{e_7}$.

2. The Jacobian matrix at $E_2 = (\hat{c}, 0,0, \hat{p}_3)$can be written as:

$$J(E_2) = \begin{bmatrix} -(\mu_0+\mu_1) & -e_1 - e_3\hat{c} & 0 & e_2 \\ 0 & -e_6\hat{p}_3 - \mu_2 & 0 & 0 \\ 0 & -r_3 & -\mu_3 & 0 \\ -r_7\hat{p}_3 & e_8\hat{p}_3 & 0 & \frac{-r_4\hat{p}_3}{m_2} \end{bmatrix}$$

Then, $J(E_2)$ has the following eigenvalues $\lambda_{22} = -(e_6\hat{p}_3 + \mu_2) < 0$, $\lambda_{23} = -\mu_3 < 0$,

$$\lambda_{21} + \lambda_{24} = -\left(\mu_0 + \mu_1 + \frac{r_4\hat{p}_3}{m_2}\right) < 0,$$

$$\lambda_{21}.\lambda_{24} = \frac{r_4\hat{p}_3}{m_2}(\mu_1+\mu_2) + e_2e_7\hat{p}_3 > 0.$$

That means E_2 is a locally asymptotical stable point.

3. The Jacobian matrix at $E_3 = (\check{c}, \check{p}_1, 0,0)$ can be written as:

$$J(E_3) = \begin{bmatrix} e_3\check{p}_1 - \mu_0 - \mu_1 & e_1 - e_3\check{c} & 0 & e_2 \\ 0 & \frac{r_2\check{p}_1[2m_1(e_4+\check{p}_1) - \check{p}_1(2\check{p}_1+3e_4)]}{m_1(e_4+\check{p}_1)^2} - \mu_2 & e_5\check{p}_1 & -e_6\check{p}_1 \\ 0 & -r_3 & -\mu_3 & 0 \\ 0 & 0 & 0 & r_4 - e_7\check{c} + e_8\check{p}_1 \end{bmatrix}.$$

Then, $J(E_3)$ has the eigenvalues
$\lambda_{31} = e_3\check{p}_1 - \mu_0 - \mu_1$,

$\lambda_{34} = r_4 + e_8\check{p}_1 - e_7\check{c}$,

$$\lambda_{32} + \lambda_{33} = \frac{r_2\check{p}_1[2m_1(e_4+\check{p}_1) - \check{p}_1(2\check{p}_1+3e_4)]}{m_1(e_4+\check{p}_1)^2} - \mu_2 - \mu_3$$

$$\lambda_{32}.\lambda_{33} = \frac{-\mu_3\check{p}_1 r_2[2m_1(e_4+\check{p}_1) - \check{p}_1(2\check{p}_1+3e_4)]}{m_1(e_4+\check{p}_1)^2} + \mu_2\mu_3 + r_3e_5\check{p}_1,$$

That means E_3 is a locally asymptotical stable point provided that:

$$\left.\begin{array}{l} \check{p}_1 < min.\left\{\frac{\mu_0+\mu_1}{e_3}, \frac{e_7\check{c}-r_3}{e_8}\right\} \\ 2m_1(e_4+\check{p}_1) < \check{p}_1(2\check{p}_1+3e_4) \end{array}\right\} \quad 8$$

4. The Jacobian matrix at $E_4 = (\bar{c}, 0, \bar{p}_2, \bar{p}_3)$ can be written as:

$$J(E_4) = \begin{bmatrix} -\mu_0 - \mu_1 & e_1 - e_3\bar{c} & 0 & e_2 \\ 0 & e_5\bar{p}_2 - e_6\bar{p}_3 - \mu_2 & 0 & 0 \\ 0 & -r_3 & -\mu_3 & 0 \\ -e_7\bar{p}_3 & e_8\bar{p}_3 & 0 & \frac{-r_4\bar{p}_3}{m_2} \end{bmatrix}.$$

Then, $J(E_4)$ has the following eigenvalues

$\lambda_{42} = e_5\bar{p}_2 - (e_6\bar{p}_3 + \mu_2)$, $\lambda_{43} = -\mu_3 < 0$,

$$\lambda_{41} + \lambda_{44} = -\left(\mu_0 + \mu_1 + \frac{r_4\bar{p}_3}{m_2}\right) < 0$$

$$\lambda_{41}.\lambda_{44} = \frac{r_4\bar{p}_3}{m_2}(\mu_0+\mu_1) + e_2e_7\bar{p}_3 > 0$$

That means E_4 is a locally asymptotical stable point provided that:

$$e_5\bar{p}_2 < e_8\bar{p}_3 + \mu_2 \quad 9$$

Published Online First: November, 2024
https://doi.org/10.21123/bsj.2024.11370
P-ISSN: 2078-8665 - E-ISSN: 2411-7986
Baghdad Science Journal

This condition states that in the absence of forest biomass, the forest-free point will be stable only if the reforestation-induced forest biomass growth coefficient is less than the human population expansion resulting from forest biomass.

5. The Jacobian matrix at $E_5 = (\ddot{c}, \ddot{p}_1, 0, \ddot{p}_3)$ can be written as:

$$J(E_5) = \begin{bmatrix} -e_3\ddot{p}_1 - \mu_0 - \mu_1 & e_1 - e_3\ddot{c} & 0 & e_2 \\ 0 & \frac{r_2\,\ddot{p}_1[2m_1(e_4+\ddot{p}_1)-\ddot{p}_1(2\ddot{p}_1+3e_4)]}{m_1(e_4+\ddot{p}_1)^2} - e_6\ddot{p}_3 - \mu_2 & e_5\ddot{p}_1 & -e_6\ddot{p}_1 \\ 0 & -r_3 & -\mu_3 & 0 \\ -e_7\ddot{p}_3 & e_8\ddot{p}_3 & 0 & \frac{-r_4\ddot{p}_3}{m_2} \end{bmatrix}.$$

Let $a_{22}^{[5]} = \frac{r_2\,\ddot{p}_1[2m_1(e_4+\ddot{p}_1)-\ddot{p}_1(2\ddot{p}_1+3e_4)]}{m_1(e_4+\ddot{p}_1)^2} - e_6\ddot{p}_3 - \mu_2$, so the characteristic equation of $J(E_5)$ can be written as:

$$\lambda^4 + {H_1}^{[5]}\lambda^3 + {H_2}^{[5]}\lambda^2 + {H_3}^{[5]}\lambda + {H_4}^{[5]} = 0,$$
here

$${H_1}^{[5]} = e_3\ddot{p}_1 + \mu_0 + \mu_1 + \mu_3 + a_{22}^{[5]} + \frac{r_4\ddot{p}_3}{m_2},$$

$${H_2}^{[5]} = -\mu_3\left(a_{22}^{[5]} - e_3\ddot{p}_1 - \mu_0 - \mu_1 - \frac{r_4\ddot{p}_3}{m_2}\right) - a_{22}^{[5]}\left(e_3\ddot{p}_1 + \mu_0 + \mu_1 + \frac{r_4\ddot{p}_3}{m_2}\right) + \frac{r_4\ddot{p}_3(e_3\ddot{p}_1 + \mu_0 + \mu_1)}{m_2} + \ddot{p}_3(e_2e_7 + e_6e_8\ddot{p}_1) + r_3e_5\ddot{p}_1,$$

$${H_3}^{[5]} = \mu_3\left(a_{22}^{[5]}\left(-e_3\ddot{p}_1 - \mu_0 - \mu_1 - \frac{r_4\ddot{p}_3}{m_2}\right) + \frac{r_4\ddot{p}_3(e_3\ddot{p}_1 + \mu_0 + \mu_1)}{m_2} + \ddot{p}_3(e_2e_7 + e_6e_8\ddot{p}_1)\right) + e_3e_6e_7\ddot{c}\ddot{p}_1\ddot{p}_3 + (e_3\ddot{p}_1 + \mu_0 + \mu_1)\left(r_3e_5\ddot{p}_1 - \frac{r_4\ddot{p}_3a_{22}^{[5]}}{m_2} + e_6e_8\ddot{p}_1\ddot{p}_3\right),$$

$${H_4}^{[5]} = -\mu_3\left(a_{22}^{[5]}\left(e_2e_7\ddot{p}_3 + \frac{r_4\ddot{p}_3(e_3\ddot{p}_1+\mu_0+\mu_1)}{m_2}\right) - e_6\ddot{p}_1\ddot{p}_3(e_3\ddot{p}_1 + \mu_0 + \mu_1 + e_3e_7\ddot{c})\right) + r_3e_5\ddot{p}_1\ddot{p}_3\left(e_2e_7 + \frac{r_4(e_3\ddot{p}_1+\mu_0+\mu_1)}{m_2}\right) - a_{22}^{[5]}e_2e_7\ddot{p}_3.$$

Now, from the Routh-Hurwitz criteria [30], E_5 is a LAS point, under the condition that

$${H_i}^{[5]} > 0, i = 1,2,3,4 \text{ and } {H_3}^{[5]}({H_1}^{[5]}{H_2}^{[5]} - {H_3}^{[5]}) - {H_1}^{2[5]}{H_4}^{[5]} > 0.$$

6. The Jacobian matrix at $E_6 = (c^*, p_1^*, p_2^*, p_3^*)$ can be written as:

$$J(E_6) = \begin{bmatrix} -e_3p_1^* - \mu_0 - \mu_1 & e_1 - e_3c^* & 0 & e_2 \\ 0 & {a_{22}}^{[6]} & e_5p_1^* & -e_6p_1^* \\ 0 & -r_3 & -\mu_3 & 0 \\ -e_7p_3^* & e_8p_3^* & 0 & \frac{-r_4p_3^*}{m_2} \end{bmatrix}$$

Let $a_{22}^{[6]} = \frac{r_2\,p_1^*[2m_1(e_4+p_1^*)-p_1^*(2p_1^*+3e_4)]}{m_1(e_4+p_1^*)^2} + e_5p_2^* - e_6p_3^* - \mu_2$, so the characteristic equation of $J(E_6)$ can be written as:

$$\lambda^4 + {H_1}^{[6]}\lambda^3 + {H_2}^{[6]}\lambda^2 + {H_3}^{[6]}\lambda + {H_4}^{[6]} = 0,$$
here

$${H_1}^{[6]} = e_3p_1^* + \mu_0 + \mu_1 + \mu_3 + a_{22}^{[6]} + \frac{r_4p_3^*}{m_2},$$

$${H_2}^{[6]} = -\mu_3\left(a_{22}^{[6]} - e_3p_1^* - \mu_0 - \mu_1 - \frac{r_3p_3^*}{m_2}\right) - a_{22}^{[6]}\left(e_3p_1^* + \mu_0 + \mu_1 + \frac{r_4p_3^*}{m_2}\right) + \frac{r_4p_3^*(e_3p_1^*+\mu_0+\mu_1)}{m_2} + p_3^*(e_2e_7 + e_6e_8p_1^*) + r_3e_5p_1^*,$$

Published Online First: November, 2024
https://doi.org/10.21123/bsj.2024.11370
P-ISSN: 2078-8665 - E-ISSN: 2411-7986
Baghdad Science Journal

$$H_3{}^{[6]} = \mu_3\left(p_3^*(e_2e_7 + e_6e_8p_1^*) - (e_3p_1^* + \mu_0 + \mu_1)a_{22}^{[6]} - \frac{r_4p_3^*}{m_2}\left(a_{22}^{[6]} - e_3p_1^* - \mu_0 - \mu_1\right)\right) + e_3e_6e_7c^*p_1^*p_3^* + (e_3p_1^* + \mu_0 + \mu_1)\left(r_3e_5p_1^* - a_{22}^{[6]}\frac{r_4p_3^*a_{22}^{[6]}}{m_2} + e_6e_8p_1^*p_3^*\right),$$

$$H_4{}^{[6]} = -\mu_3\left(\frac{r_4p_3^*(e_3p_1^*+\mu_0+\mu_1)a_{22}^{[6]}}{m_2} + a_{22}^{[6]}e_2e_7p_3^* - e_6p_1^*p_3^*(e_3p_1^* + \mu_0 + \mu_1 - e_3e_7c^*)\right) + r_3e_5p_1^*p_3^*\left(e_2e_7 + \frac{r_4(e_3p_1^*+\mu_0+\mu_1)}{m_2}\right) - a_{22}^{[6]}e_2e_7p_3^*,$$

Now, from the Routh-Hurwitz criteria, E_6 is a LAS point under the condition that

$$H_i{}^{[6]} > 0, i = 1,2,3,4 \text{ and } H_3{}^{[6]}\left(H_1{}^{[6]}H_2{}^{[6]} - H_3{}^{[6]}\right) - H_1{}^{2[6]}H_4{}^{[6]} > 0.$$

Using the Lyapunov method [30-32], the following theories look into what needs to happen for the system's (1) global stability (GS) property to be present at the points where there is no reforestation and where there is reforestation.

Theorem 3: The reforestation-free equilibrium $E_5 = (\ddot{c}, \ddot{p}_1, 0, \ddot{p}_3)$ is GAS provided the following conditions are satisfied:

$$6(e_4 + p_1)(e_4 + \ddot{p}_1)(e_1 - e_3c - e_4)^2 \le (e_3\ddot{p}_1 + \mu_1 + \mu_0)r_2\left(p_1^2 - m_2e_4 + (e_4 + p_1)(p_1 + \ddot{p}_1)\right)$$

$$4m_2(e_7 - e_2)^2 \le r_4(e_3\ddot{p}_1 + \mu_0 + \mu_1) \qquad 10$$

$$6m_2(e_4 + p_1)(e_4 + \ddot{p}_1)(e_8 + e_6)^2 \le r_4r_2\left(p_1^2 - m_2e_4 + (e_4 + p_1)(p_1 + \ddot{p}_1)\right)$$

$$3e_5^2 \le \mu_3r_2\left(p_1^2 - m_2e_4 + (e_4 + p_1)(p_1 + \ddot{p}_1)\right)$$

Proof: Let us contemplate the positive definite function given below:

$$W_5 = \frac{(c-\ddot{c})^2}{2} + \left(p_1 - \ddot{p}_1 - \ddot{p}_1\ln\frac{p_1}{\ddot{p}_1}\right) + p_2 + \left(p_3 - \ddot{p}_3 - \ddot{p}_3\ln\frac{p_3}{\ddot{p}_3}\right).$$

Thus,

$$\frac{dW_5}{dt} = (e_1 - e_3c)(c - \ddot{c})(p_1 - \ddot{p}_1) + (e_2 - e_7)(p_3 - \ddot{p}_3)(c - \ddot{c}) - (\mu_0 + \mu_1 - e_3\ddot{p}_1)(c - \ddot{c})^2 + (p_1 - \ddot{p}_1)^2\left(\frac{r_2\left(m_2e_4 - p_1^2 - (e_4+p_1)(p_1+\ddot{p}_1)\right)}{(e_4+p_1)(e_4+\ddot{p}_1)}\right) + e_5p_2(p_1 - \ddot{p}_1) - e_6(p_3 - \ddot{p}_3)(p_1 - \ddot{p}_1) + r_3m_1 - r_3p_1 - \mu_3p_2 - \frac{r_4}{m_2}(p_3 - \ddot{p}_3)^2 + e_8(p_1 - \ddot{p}_1)(p_3 - \ddot{p}_3).$$

Therefore,

$$\frac{dW_5}{dt} \le -\left[\sqrt{\frac{\mu_0+\mu_1-e_3\ddot{p}_1}{2}}(c - \ddot{c}) + \sqrt{\left(\frac{r_2\left(p_1^2-m_2e_4+(e_4+p_1)(p_1+p_1^*)\right)}{3(e_4+p_1)(e_4+p_1^*)}\right)}(p_1 - \ddot{p}_1)\right]^2 - \left[\sqrt{\frac{\mu_0+\mu_1-e_3\ddot{p}_1}{2}}(c - \ddot{c}) + \sqrt{\frac{r_4}{2m_2}}(p_3 - \ddot{p}_3)\right]^2 - \left[\sqrt{\frac{r_4}{2m_2}}(p_3 - \ddot{p}_3) + \sqrt{\left(\frac{r_2\left(p_1^2-m_2e_4+(e_4+p_1)(p_1+p_1^*)\right)}{3(e_4+p_1)(e_4+p_1^*)}\right)}(p_1 - \ddot{p}_1)\right]^2 - \left[\sqrt{\mu_3p_2} + \sqrt{\left(\frac{r_2\left(p_1^2-m_2e_4+(e_4+p_1)(p_1+p_1^*)\right)}{3(e_4+p_1)(e_4+p_1^*)}\right)}(p_1 - \ddot{p}_1)\right]^2 + r_3(m_1 - p_1).$$

Then, $\frac{dW_5}{dt} < 0$ can be transformed into a negative definite form under conditions (10). Hence, W_5 is a Lyapunov function and E_5 is a GAS.

Published Online First: November, 2024
https://doi.org/10.21123/bsj.2024.11370
P-ISSN: 2078-8665 - E-ISSN: 2411-7986
Baghdad Science Journal

Theorem 4: The reforestation equilibrium $E_6 = (c^*, p_1^*, p_2^*, p_3^*)$ is GAS if the following conditions are satisfied:

$$6(e_1 - e_3 c)^2 (e_4 + p_1)(e_4 + p_1^*) \le (\mu_1 + \mu_0 - e_3 p_1^*)(r_2\left(m_2 e_4 - p_1^2 - (e_4 + p_1)(p_1 + p_1^*)\right).$$

$$4m_2(e_2 - e_7)^2 \le r_4(\mu_1 + \mu_0 - e_3 p_1^*). \qquad 11$$

$$3(e_5 - r_3)^2 (e_4 + p_1)(e_4 + p_1^*) \le \mu_3(r_2\left(m_2 e_4 - p_1^2 - (e_4 + p_1)(p_1 + p_1^*)\right).$$

$$6m_2(e_6 - e_8)^2 \le r_4(r_2\left(m_2 e_4 - p_1^2 - (e_4 + p_1)(p_1 + p_1^*)\right).$$

Proof: Define $W_6 = \frac{(c-c^*)^2}{2} + \left(p_1 - p_1^* - p_1^* \ln\frac{p_1}{p_1^*}\right) + \left(\frac{p_2 - p_2^*}{2}\right) + \left(p_3 - p_3^* - p_3^* \ln\frac{p_3}{p_3^*}\right)$, where $W_6(c, p_1, p_2, p_3)$ is a positive definite function about E_6. Thus,

$$\frac{dW_6}{dt} = e_1(c - c^*)(p_1 - p_1^*) + e_2(p_3 - p_3^*)(c - c^*) - e_3 c(c - c^*)(p_1 - p_1^*) + e_3 p_1^*(c - c^*)^2 - (\mu_0 + \mu_1)(c - c^*)^2 + \frac{r_2\left(m_2 e_4 - p_1^2 - (e_4 + p_1)(p_1 + p_1^*)\right)}{(e_4 + p_1)(e_4 + p_1^*)}(p_1 - p_1^*)^2 + e_5(p_1 - p_1^*)(p_2 - p_2^*) - e_6(p_1 - p_1^*)(p_3 - p_3^*) - r_3(p_1 - p_1^*)(p_2 - p_2^*) - \mu_3(p_2 - p_2^*)^2 - \frac{r_4}{m_2}(p_3 - p_3^*)^2 - e_7(p_3 - p_3^*)(c - c^*) + e_8(p_1 - p_1^*)(p_3 - p_3^*).$$

Therefore,

$$\frac{dW_6}{dt} \le -\left(\sqrt{\frac{\mu_0 + \mu_1 - e_3 p_1^*}{2}}(c - c^*) + \sqrt{\frac{r_2\left(p_1^2 - m_2 e_4 + (e_4 + p_1)(p_1 + p_1^*)\right)}{3(e_4 + p_1)(e_4 + p_1^*)}}(p_1 - p_1^*)\right)^2 - \left(\sqrt{\frac{\mu_1 + \mu_0 - e_3 p_1^*}{2}}(c - c^*) + \sqrt{\frac{r_4}{2m_2}}(p_3 - p_3^*)\right)^2 - \left(\sqrt{\mu_3}(p_2 - p_2^*) + \sqrt{\frac{r_2\left(p_1^2 - m_2 e_4 + (e_4 + p_1)(p_1 + p_1^*)\right)}{3(e_4 + p_1)(e_4 + p_1^*)}}(p_1 - p_1^*)\right)^2 - \left(\sqrt{\frac{r_4}{2m_2}}(p_3 - p_3^*) + \sqrt{\frac{r_2\left(p_1^2 - m_2 e_4 + (e_4 + p_1)(p_1 + p_1^*)\right)}{3(e_4 + p_1)(e_4 + p_1^*)}}(p_1 - p_1^*)\right)^2.$$

Then, $\frac{dW_6}{dt} < 0$ under condition (11). Hence, W_6 is a Lyapunov function and E_6 is a GAS.

Local bifurcation

A transcritical split occurs when two equilibrium points collide and exchange their stability. The following theorems will investigate the possibility of a transcritical split occurring. Many scholars use Sotomayor's theorem to determine the existence of transcritical bifurcation TB; for instance, see[33-35]. For this determination, the system (1) can be rephrased in the following vector forms:

$$\frac{dE}{dt} = F(E) \text{ with } E = \begin{pmatrix} c \\ p_1 \\ p_2 \\ p_3 \end{pmatrix}, \text{ and } F = \begin{pmatrix} f_1(c, p_1, p_3) \\ f_2(p_1, p_2, p_3) \\ f_3(p_1, p_2) \\ f_4(c, p_1, p_3) \end{pmatrix},$$

The subsequent outcomes concerning the local bifurcation around each equilibrium point.

Theorem 5: For $e_7{}^* = \frac{r_3(\mu_0 + \mu_1)}{r_1}$, system (1) at E_1 has a transcritical bifurcation (TB).

Proof: At $e_7{}^* = \frac{r_4(\mu_1 + \mu_0)}{r_1}$, $J(E_1)$ has a zero eigenvalue $\lambda_{14} = 0$. Therefore, $J(E_1)$ at $e_7{}^*$ becomes

Published Online First: November, 2024
https://doi.org/10.21123/bsj.2024.11370
P-ISSN: 2078-8665 - E-ISSN: 2411-7986
Baghdad Science Journal

$$J^*(E_1)=\begin{pmatrix}-\mu_0-\mu_1 & e_1-\frac{e_3r_1}{\mu_0+\mu_1} & 0 & e_2\\ 0 & -\mu_2 & 0 & 0\\ 0 & -r_3 & -\mu_3 & 0\\ 0 & 0 & 0 & 0\end{pmatrix}.$$

Now, let $V^{[1]}=\left(v_1{}^{[1]},v_2{}^{[1]},v_3{}^{[1]},v_4{}^{[1]}\right)^T$ and $(T^{[1]})^T=\left(t_1{}^{[1]},t_2{}^{[1]},t_3{}^{[1]},t_4{}^{[1]}\right)^T$ represent the eigenvectors corresponding to the zero eigenvalue of $J^*(E_1)$ and $J^{*T}(E_1)$ respectively. Direct computation gives $V^{[1]}=\left(\frac{e_2}{\mu_0+\mu_1},0,0,1\right)$ and $T^{[1]}=(0,0,0,1)$. Then

$$T^{[1]^T}F_{e_7}(E_1,e_7^*)=(0,0,0,1)(0,0,0,0)^T=0.$$

$$\left(T^{[1]}\right)^T DF_{e_7}(E_1,e_7^*)V^{[1]}=(0,0,0,1)\begin{pmatrix}0&0&0&0\\0&0&0&0\\0&0&0&0\\0&0&0&-\tilde{c}\end{pmatrix}\left(\frac{e_2}{\mu_0+\mu_1},0,0,1\right)^T=-\tilde{c}\neq 0.$$

$$(T^{[1]})^T\left[D^2F(E_1,e_7{}^*)\left(V^{[1]},V^{[1]}\right)\right]=(0,0,0,1)\left(0,0,0,-2e_7v_1^{[1]}-\frac{2r_2}{m_1}\right)^T=-2e_7v_1^{[1]}-\frac{2r_2}{m_1}\neq 0.$$

This means the required conditions to have TB are satisfied.

Theorem 6: For $r_2^*=\frac{m_1(e_4+\check{p}_1)^2(\mu_2+\mu_3)}{\check{p}_1[2m_1(e_4+\check{p}_1)-\check{p}_1(2\check{p}_1+3e_4)]}$, system (1) at E_3 has a TB if the following are satisfied

$$\left.\begin{array}{c}\check{p}_1=m_1\\ 2m_1(e_4+p_1)\neq p_1(2p_1+3e_4)\\ (T^{[3]})^T\left[D^2E(E_3,r_2{}^*)\left(V^{[3]},V^{[3]}\right)\right]\neq 0\end{array}\right\} \quad 12$$

Proof: at $r_2^*=\frac{m_1(e_4+\check{p}_1)^2(\mu_2+\mu_3)}{\check{p}_1[2m_1(e_4+\check{p}_1)-\check{p}_1(2\check{p}_1+3e_4)]}$, where $r_2^*>0$, $J(E_3)$ has zero eigenvalues $\lambda_{34}=0$. The Jacobian matrix at r_2^* becomes:

$$J^*(E_3)=\begin{pmatrix}e_3\check{p}_1-\mu_0-\mu_1 & e_1-e_3\check{c} & 0 & e_2\\ 0 & c_{22}{}^{[3]} & e_5\check{p}_1 & -e_6\check{p}_1\\ 0 & -r_3 & -\mu_3 & 0\\ 0 & 0 & 0 & r_4-e_7\check{c}+e_8\check{p}_1\end{pmatrix},$$

Where,

$c_{22}{}^{[3]}=\frac{r_2^*\check{p}_1[2m_1(e_4+\check{p}_1)-\check{p}_1(2\check{p}_1+3e_4)]}{m_1(e_4+\check{p}_1)^2}-\mu_2$. Now, let $V^{[3]}=\left(v_1{}^{[3]},v_2{}^{[3]},v_3{}^{[3]},v_4{}^{[3]}\right)$ and $(T^{[3]})^T=\left(t_1{}^{[3]},t_2{}^{[3]},t_3{}^{[3]},t_4{}^{[3]}\right)^T$ represent the eigenvectors corresponding to the zero eigenvalue of $J^*(E_3)$ and $J^{*T}(E_3)$ respectively. Direct computation gives $V^{[3]}=\left(1,1,\frac{-r_3}{\mu_3},0\right)$ and $T^{[3]}=\left(0,1,\frac{e_5\check{p}_1}{\mu_3},\frac{e_6\check{p}_1}{r_4-e_7\check{c}+e_8\check{p}_1}\right)$. Then

$$\left(T^{[3]}\right)^T F_{r_2}(E_3,r_2^*)=\left(0,1,\frac{e_5\check{p}_1}{\mu_3},\frac{e_6\check{p}_1}{r_4-e_7\check{c}+e_8\check{p}_1}\right)\left(0,\left(1-\frac{\check{p}_1}{m_1}\right)\left(\frac{\check{p}_1^2}{e_4+\check{p}_1}\right),0,0\right)^T=\left(1-\frac{\check{p}_1}{m_1}\right)\left(\frac{\check{p}_1^2}{e_4+\check{p}_1}\right).$$

$$\left(T^{[3]}\right)^T\left[DF_{r_2}(E_3,r_2^*)V^{[3]}\right]=\frac{p_1[2m_1(e_4+p_1)-p_1(2p_1+3e_4)]}{m_1(e_4+p_1)^2}.$$

$$(T^{[3]})^T\left[D^2F(E_3,r_2{}^*)\left(V^{[3]},V^{[3]}\right)\right]=\frac{2r_2^*\left(e_4p_1\left(e_4m_1-4p_1^2-3e_4^2-6e_4p_1\right)-p_1^4+e_4^3m_1\right)}{m_1(e_4+p_1)^4}+2e_5v_3.$$

This means the required conditions for TB are satisfied if the conditions stated in Eqs.12 are met.

Theorem 7: For $\mu_2^*=e_4\bar{c}+e_5\bar{p}_2-e_6\bar{p}_3$, system (1) at E_4 has a TB if

$$(T^{[4]})^T\left[D^2E(E_4,\mu_2{}^*)\left(V^{[4]},V^{[4]}\right)\right]\neq 0. \quad 13$$

Proof: at $\mu_2^*=e_4\bar{c}+e_5\bar{p}_2-e_6\bar{p}_3, J(E_4)$ has zero eigenvalues $\lambda_{42}=0$. The Jacobian matrix at μ_2^* becomes:

Published Online First: November, 2024
https://doi.org/10.21123/bsj.2024.11370
P-ISSN: 2078-8665 - E-ISSN: 2411-7986
Baghdad Science Journal

$$J^*(E_4)=\begin{pmatrix}-\mu_0-\mu_1 & e_1-e_3\bar{c} & 0 & e_2\\ 0 & 0 & 0 & 0\\ 0 & -r_3 & -\mu_3 & 0\\ -e_7\bar{p}_3 & e_8\bar{p}_3 & 0 & \dfrac{-r_4\bar{p}_3}{m_2}\end{pmatrix}$$

Now, $V^{[4]}=\left(1,1,\frac{-r_3}{\mu_3},\frac{(\mu_0+\mu_1)-(e_1-e_3\bar{c})}{e_2}\right)$ and $T^{[4]}=\left(1,1,0,\frac{-(\mu_1+\mu_0)}{e_7\bar{p}_3}\right)$ represent the eigenvectors corresponding to the zero eigenvalue of $J^*(E_4)$ and $J^{*T}(E_4)$ respectively. Then, direct computation gives

$$\left(T^{[4]}\right)^T F_{\mu_1}(E_4,\mu_2^*)=\left(1,1,0,\frac{-(\mu_1+\mu_0)}{e_7\bar{p}_3}\right)(0,0,0,0)^T=0$$

$$\left(T^{[4]}\right)^T\left[DF_{\mu_2}(E_4,\mu_2^*)V^{[4]}\right]=\left(1,1,0,\frac{-(\mu_1+\mu_0)}{e_7\bar{p}_3}\right)^T(0,-1,0,0)=-1\neq 0$$

$$\left(T^{[4]}\right)^T\left[D^2F(E_4,{\mu_2}^*)\left(V^{[4]},V^{[4]}\right)\right]=-2e_3+x_{21}^{[4]}+\frac{2(\mu_0+\mu_1)}{m_2e_7}\left(m_2v_4^{[4]}(e_7-e_8)+r_3\right).$$

This means the required conditions for TB are satisfied if the conditions stated in (13) are met.

Theorem 8: For $e_5=e_5^*$, at the equilibrium point E_5 has a TB if

$$(T^{[5]})^T\left[D^2E(E_5,e_5^*)\left(V^{[5]},V^{[5]}\right)\right]\neq 0 \quad 14$$

Proof: System (1) at $e_5=\frac{{H_3}^{[5]}\left({H_1}^{[5]}{H_2}^{[5]}-{H_3}^{[5]}\right)}{b_2^{[5]}r_3\ddot{p}_1\ddot{p}_3H_1^{2[5]}}-b_1^{[5]}$, where $e_5>0$ and

$$b_1^{[5]}=\mu_3\left(a_{22}^{[5]}\left(e_2e_7\ddot{p}_3+\frac{r_4\ddot{p}_3(e_3\ddot{p}_1+\mu_0+\mu_1)}{m_2}\right)-e_6\ddot{p}_1\ddot{p}_3(e_3\ddot{p}_1+\mu_0+\mu_1+e_3e_7\ddot{c})\right)+a_{22}^{[5]}e_2e_7\ddot{p}_3.$$

$b_2^{[5]}=e_2e_7+\frac{r_4(e_3\ddot{p}_1+\mu_0+\mu_1)}{m_2}$, has a zero-eigenvalue if

$$\Delta_2={H_3}^{[5]}\left({H_1}^{[5]}{H_2}^{[5]}-{H_3}^{[5]}\right)-{H_1}^{2[5]}{H_4}^{[5]}=0,$$

where $a_{22}^{[5]}$ and H_i are given in the local stability analysis of E_5. Now, the Jacobian matrix $J(E_5)=J(E_5,e_5^*)$, becomes

$$J^*(E_5)=\begin{pmatrix}-e_3\ddot{p}_1-\mu_0-\mu_1 & e_1-e_3\ddot{c} & 0 & e_2\\ 0 & {c_{22}}^{[5]} & e_5^*\ddot{p}_1 & -e_6\ddot{p}_1\\ 0 & -r_3 & -\mu_3 & 0\\ -e_7\ddot{p}_3 & e_8\ddot{p}_3 & 0 & \dfrac{-r_4\ddot{p}_3}{m_2}\end{pmatrix},$$

Now, $V^{[5]}=\left(1,1,\frac{-r_3}{\mu_3},\frac{(e_3\ddot{p}_1+\mu_0+\mu_1)-(e_1-e_3\ddot{c})}{e_2}\right)$ and $T^{[5]}=\left(1,1,\frac{e_5^*\ddot{p}_1}{\mu_3},\frac{-(e_3\ddot{p}_1+\mu_0+\mu_1)}{-e_7\ddot{p}_3}\right)$ represent the eigenvectors corresponding to the zero eigenvalue of $J^*(E_5)$ and $J^{*T}(E_5)$ respectively. Then, direct computation gives

$$\left(T^{[5]}\right)^T F_{e_5}(E_5,e_5^*)=\left(1,1,\frac{e_5^*\ddot{p}_1}{\mu_3},\frac{-(e_3\ddot{p}_1+\mu_0+\mu_1)}{-e_7\ddot{p}_3}\right)(0,0,0,0)^T=0$$

$$\left(T^{[5]}\right)^T\left[DF_{e_5}(E_5,e_5^*)V^{[5]}\right]=\left(1,1,0,\frac{-(\mu_1+\mu_0)}{e_7\bar{p}_3}\right)^T\left(0,\ddot{p}_1v_3^{[5]},0,0\right)=\ddot{p}_1v_3^{[5]}\neq 0$$

$$\left(T^{[5]}\right)^T\left[D^2F_{e_5}(E_5,e_5^*)\left(V^{[5]},V^{[5]}\right)\right]=-2e_3+x_{21}^{[4]}+\frac{2(\mu_0+\mu_1)}{m_2e_7}\left(m_2v_4^{[4]}(e_7-e_8)+r_3\right).$$

This means the required conditions for TB are satisfied if the conditions stated in (14) are met.

Now, the following theorems examine the criteria that determine the appearance of a Hopf bifurcation around E_5 and E_6 using Haque and Venturino methods [36,38].

Theorem 9: Suppose that the following conditions are satisfied

$$H_i^{[5]}>0, i=1,3$$

Published Online First: November, 2024
https://doi.org/10.21123/bsj.2024.11370
P-ISSN: 2078-8665 - E-ISSN: 2411-7986
Baghdad Science Journal

$$\Delta_1^{[5]} = H_1{}^{[5]} H_2{}^{[5]} - H_3{}^{[5]} > 0 \qquad 16$$

$$e_7^* > 0, \qquad 17$$

$$\theta(e_7^*)\psi(e_7^*) + \Gamma(e_7^*)\phi(e_7^*) \neq 0 \qquad 18$$

Where the formula of e_7^*, $\theta(e_7^*), \psi(e_7^*), \Gamma(e_7^*)$ and $\phi(e_7^*)$ are given in the following proof. Then, the system has a Hope bifurcation at $e_7 = e_7^*$ around E_5.

Proof: To verify the necessary and sufficient conditions for Hope bifurcation to occur at E_5, it needs to find a parameter such that $H_3{}^{[5]}\left(H_1{}^{[5]} H_2{}^{[5]} - H_3{}^{[5]}\right) - H_1{}^{2[5]} H_4{}^{[5]} = 0$. It is observed that $H_3{}^{[5]}\left(H_1{}^{[5]} H_2{}^{[5]} - H_3{}^{[5]}\right) - H_1{}^{2[5]} H_4{}^{[5]} = 0$ gives $e_7^* = \frac{H_3^{2[6]} + H_1^{2[6]} H_4^{[6]}}{e_2 p_3^* H_1^{[6]} H_3^{[6]}} - e_2 p_3^* b^{[5]}$, where,

$$b^{[5]} = -\mu_3\left(a_{22}^{[5]} - e_3 \ddot{p}_1 - \mu_0 - \mu_1 - \frac{r_4 \ddot{p}_3}{m_2}\right) - a_{22}^{[5]}\left(e_3 \ddot{p}_1 + \mu_0 + \mu_1 + \frac{r_4 \ddot{p}_3}{m_2}\right) + \frac{r_4 \ddot{p}_3 (e_3 \ddot{p}_1 + \mu_0 + \mu_1)}{m_2}$$
$$+ e_6 e_8 \ddot{p}_1 \ddot{p}_3 + r_3 e_5 \ddot{p}_1.$$

Clearly $e_7^* > 0$ provided condition 17 holds. Now at $e_7 = e_7^*$, the characteristic equation given in the local stability analysis of E_5 can be written as:

$$\left(\lambda^2 + \frac{H_3^{[5]}}{H_1^{[5]}}\right)\left(\lambda^2 + H_1^{[5]}\lambda + \frac{\Delta_1^{[5]}}{H_1^{[5]}}\right) = 0, \qquad 19$$

which has four roots

$$\lambda_{1,2} = \pm i\sqrt{\frac{H_3^{[5]}}{H_1^{[5]}}}\ ,\ \lambda_{3,4} = \frac{1}{2}\left(-H_1^{[5]} \pm \sqrt{H_1^{2[5]} - 4\frac{\Delta_1^{[5]}}{H_1^{[5]}}}\right)$$

Clearly, at $e_7 = e_7^*$ there are two purely imaginary eigenvalues λ_1 and λ_2 and two eigenvalues λ_3 and λ_4 which have negative real parts provided conditions 15-16 hold. Now, for all values of e_7 in the neighborhood of e_7^*, the roots, in general, have the following forms:

$$\lambda_{1,2} = \alpha_1 \pm i\alpha_2,$$
$$\lambda_{3,4} = \frac{1}{2}\left(-H_1^{[5]} \pm \sqrt{H_1^{2[5]} - 4\frac{\Delta_1^{[5]}}{H_1^{[5]}}}\right).$$

Clearly at $e_7 = e_7^*$, $Re(\lambda_{1,2})|_{e_7 = e_7^*} = \alpha_1(e_7^*) = 0$, which means fulfilling the first condition for Hopf bifurcation implies that the necessary condition is followed. To validate the transversality condition, $\alpha_1 \pm i\alpha_2$ is substituted into Eq 19 and then calculate its derivative concerning e_7 , and compute the form $\theta(e_7^*)\psi(e_7^*) + \Gamma(e_7^*)\phi(e_7^*)$ where the form of θ, ψ, Γ and ϕ are

$$\theta(e_7) = \left(\alpha_1(e_7)\right)^3 H_1'^{[5]}(e_7) + \alpha_1(e_7) H_3'^{[5]}(e_7) + \left(\alpha_1(e_7)\right)^2 H_2'(e_7)^{[5]} + H_4'^{[5]}(e_7) - 3\alpha_1(e_7)\left(\alpha_2(e_7)\right)^2 H_1'^{[5]}(e_7) - \left(\alpha_2(e_7)\right)^2 H_2'(e_7)^{[5]}.$$

$$\Gamma(e_7) = 3\left(\alpha_1(e_7)\right)^2 \alpha_2(e_7) H_1'^{[5]}(e_7) + \alpha_2(e_7) H_3'^{[5]}(e_7) + 2\alpha_1(e_7)\alpha_2(e_7) H_2'^{[5]}(e_7) - \alpha_2(e_7) H_1'^{[5]}(e_7).$$

$$\psi(e_7) = 4\left(\alpha_1(e_7)\right)^3 + 3\left(\alpha_1(e_7)\right)^2 H_1^{[5]}(e_7) + H_3^{[5]}(e_7) + 2\alpha_2(e_7) H_2^{[5]}(e_7) - 12\alpha_1(e_7)\left(\alpha_2(e_7)\right)^2 - 3\left(\alpha_2(e_7)\right)^2 H_1'^{[5]}(e_7).$$

$$\phi(e_7) = 12\left(\alpha_1(e_7)\right)^2 \alpha_2(e_7) + 6\alpha_1(e_7)\alpha_2(e_7) H_1^{[5]}(e_7) + 2\alpha_2(e_7) H_2^{[5]}(e_7) - 4\left(\alpha_2(e_7)\right)^3.$$

Then, for $e_7 = e_7^* \Rightarrow \alpha_1 = 0$, $\alpha_2 = \sqrt{\frac{H_3^{[5]}}{H_1^{[5]}}}$ and

$$\theta(e_7^*) = H_4'^{[5]}(e_7^*) - \frac{H_2'^{[5]}(e_7^*) H_3^{[5]}(e_7^*)}{H_1^{[5]}(e_7^*)}, \qquad \Gamma(e_7^*) = \alpha_2(e_7^*)\left[H_3^{[5]}(e_7^*) - \frac{H_1'^{[5]}(e_7^*) H_3^{[5]}(e_7^*)}{H_1^{[5]}(e_7^*)}\right],$$

$\psi(e_7^*) = -2H_3^{[5]}(e_7^*)$, $\phi(e_7^*) = \frac{2\alpha_2(e_7^*)}{H_1^{[5]}(e_7^*)}\left[H_2^{[5]}(e_7^*)H_1^{[5]}(e_7^*) - 2H_3^{[5]}(e_7^*)\right]$.

Hence, according to condition 18, the following is obtained.

$\theta(e_7^*)\psi(e_7^*) + \Gamma(e_7^*)\phi(e_7^*) = 2H_3^{[5]}(e_7^*)\left[\ddot{p}_3\left(\mu_3 e_2 a_{22}^{[5]} - e_3 e_6 \ddot{c}\ddot{p}_1 - r_3 e_2 e_5 \ddot{p}_1 + e_2 a_{22}^{[5]} + \frac{e_2 H_3^{[5]}}{H_1^{[5]}}\right) + \frac{\alpha_2^2(e_7^*)}{H_1^{[5]}(e_7^*)}\left[H_2^{[5]}(e_7^*)H_1^{[5]}(e_7^*) - 2H_3^{[5]}(e_7^*)\right]\right] \neq 0$. This means the required conditions for HB are satisfied.

Results and Discussion

In this section, MATLAB is utilized to conduct numerical simulations of a system (1) to demonstrate the outcomes derived from our theoretical study. The data set below displays a set of ecologically feasible parameter values that have been considered [19].

$$r_1 = 1;\ e_1 = 0.002;\ e_2 = 0.15;\ e_3 = 0.03;\ e_4 = 0.001;\ e_5 = 0.0001;\ e_6 = 0.0002;\ e_7 = 0.001;$$

$$e_8 = 0.002;\ r_2 = 0.25;\ r_3 = 0.01;\ r_4 = 0.2;\ m_1 = 1000;\ m_2 = 20000;\ \mu_0 = 0.0002;\ \mu_1 = 0.0001;$$

$$\mu_2 = 0.02;\ \mu_3 = 0.02 \qquad 21$$

To understand the dynamic behavior of system (1) and evaluate the impact of reforestation on CO_2 emissions, two scenarios are examined. The results of the two cases will then be juxtaposed to facilitate comparison. The two cases are:

- **The system without reforestation**

In this case, the interaction dynamics between the carbon dioxide concentration $c(t)$, the forest biomass $p_1(t)$, and the human population density $p_3(t)$ in the absence of reforestation efforts, i.e., where $r_3 = \mu_3 = 0$ is examined. Fig 2 depicts the system (1) model with a reforestation-free equilibrium point $E_5 = (2, 0, 2.38, 0)$. Moreover, despite the initial values, the solution undergoes an initial phase of expansion or contraction before reaching E_5 in an asymmetrical convergence direction. Every condition necessary for the existence and global stability of $E_5 = (352.94,170.2,0,943.98)$ is fulfilled.

Theorem 10: Suppose that the following conditions are satisfied

$$\left.\begin{array}{c} H_i^{[6]} > 0, i = 1,3 \\ \Delta_1^{[6]} = H_1{}^{[6]}H_2{}^{[6]} - H_3{}^{[6]} > 0 \\ e_8^* > 0 \\ \theta(e_8^*)\psi(e_8^*) + \Gamma(e_8^*)\phi(e_8^*) \neq 0 \end{array}\right\}, \qquad 20$$

Then, system (1) has a Hopf bifurcation at $e_8 = e_8^*$ around E_6.

Proof: the proof is similar to Theorem 9, hence omitted.

Published Online First: November, 2024
https://doi.org/10.21123/bsj.2024.11370
P-ISSN: 2078-8665 - E-ISSN: 2411-7986

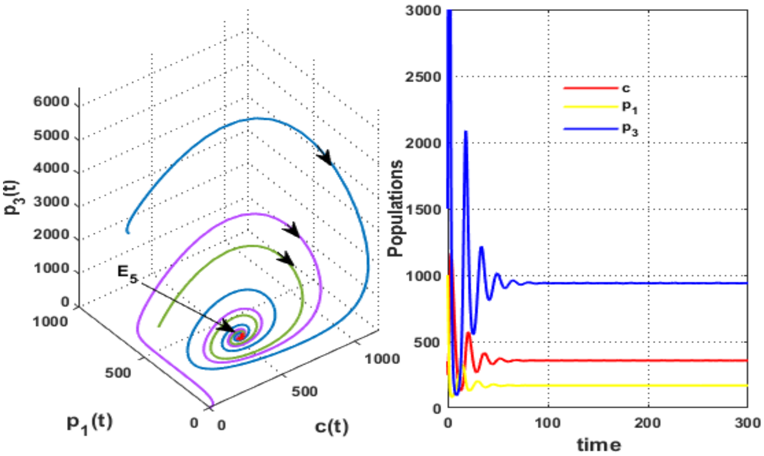

Figure 2. The existence and global stability for the parameters given in (21) with $r_3 = \mu_3 = 0$.

Fig 3 illustrates the increase in the coefficient of natural depletion of forest biomass (μ_2), which ultimately leads to a reduction in both human and forest populations and rising in the CO_2 in the atmosphere. The system, in this case, settles down to the CO_2 equilibrium point $E_1 = (824.96, 0, 0, 0)$ for $\mu_2 \geq 0.26$.

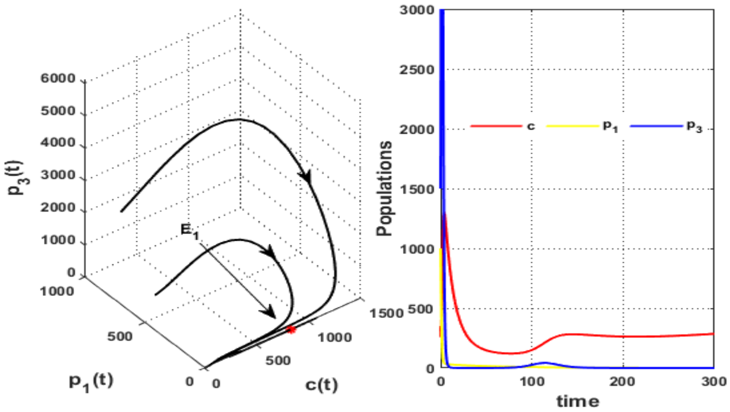

Figure 3. The existence and global stability for the parameters given in (21) with $\mu_2 = 0.26$.

To assess the impact of the coefficient of CO_2 uptake by forest biomass as a result of photosynthesis (e_3). System (1) was solved using the dataset presented in (21) with varying values of e_3. The result shows for $e_3 \leq 0.00001$ the human population faces extinction, and system (1), in this case, approaches asymptotically to the carbon dioxide gas-forest equilibrium point $E_3 = (\check{c}, \check{p}_1, 0,0) = (22378.9, 920,0,0)$. Furthermore, the decrease in the coefficient of CO_2 uptake by forest biomass due to photosynthesis results in a significant rise in the amount of CO_2 in the environment. See Fig 4.

Published Online First: November, 2024
https://doi.org/10.21123/bsj.2024.11370
P-ISSN: 2078-8665 - E-ISSN: 2411-7986
Baghdad Science Journal

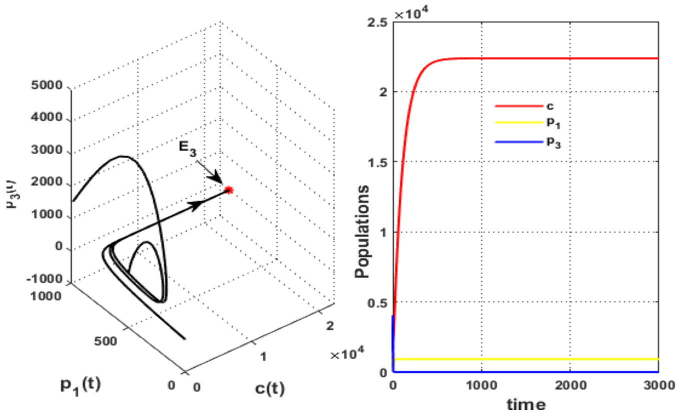

Figure 4. The existence and global stability for the parameters given in (21) with $e_3 = 0.00001$.

The impact of the reduction in the intrinsic growth rate of the forest biomass (r_2) is shown in Fig 5. It shows a comprehensive bifurcation diagram with r_2 representing the bifurcation point. It is evident from the diagram that the system undergoes two transcritical bifurcations: when the CO_2 equilibrium point E_1 and the carbon dioxide gas-forest equilibrium point E_3 exchange their stability. It is clear from Fig 5 that for a small value of $r_2 \leq 0.12$, for example if $r_2 = 0.02$, system (1) settles down asymptotically to $E_1 = (750.12,0,0,0)$. Moreover, to raise the value of r_2 (say $r_2 = 0.14$), it is observed that system (1) approaches asymptotically to $E_3 = (\check{c}, \check{p}_1, 0,0) = (104.19, 11.65,0,0)$. Therefore, the conditions stated in theorem 6 are satisfied, and system (1) faces a transcritical bifurcation at $r_2^* = 0.12$. The result shows that a decrease in r_2 harms both the forest and human populations and causes an increase in the amount of CO_2 in the environment.

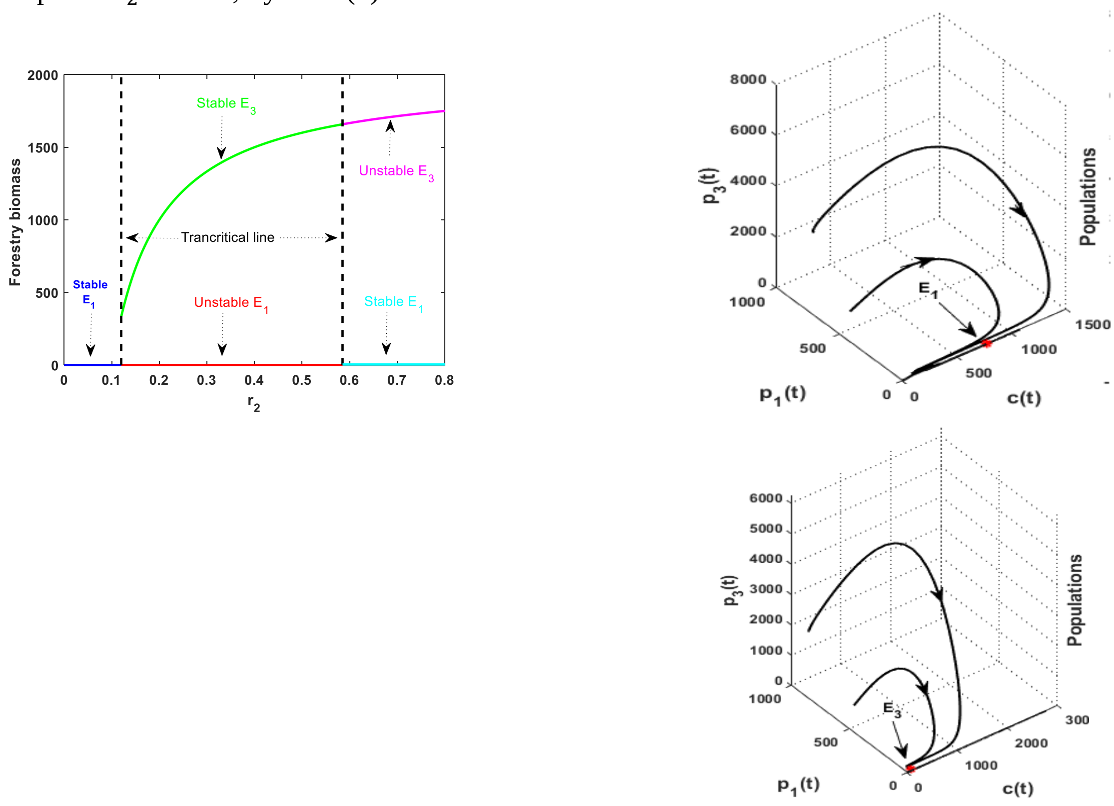

Figure 5. Transcritical bifurcation with respect to r_2.

Published Online First: November, 2024
https://doi.org/10.21123/bsj.2024.11370
P-ISSN: 2078-8665 - E-ISSN: 2411-7986
Baghdad Science Journal

Now, numerically verifies the effect of the coefficient of CO_2 emission from anthropogenic sources (e_2). Fig 6 illustrates that for $0.001 < e_2 \leq 0.01$, the solution faces a periodic attractor. While it settles down to the CO_2 equilibrium point $E_1 = (2041.03, 0, 0, 0)$ for $e_2 \leq 0.001$. See Fig 7.

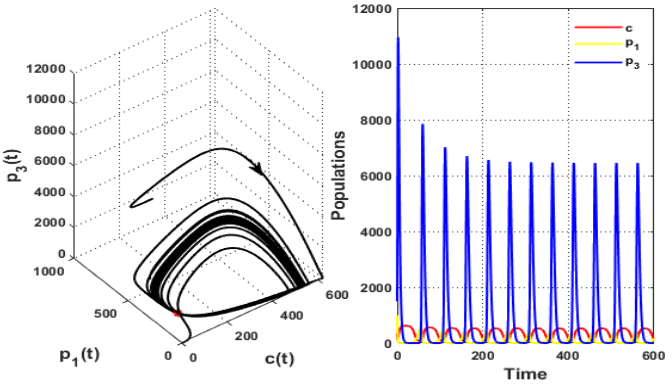

Figure 6. The existence of a periodic attractor for the dataset given in (21) with $e_2 = 0.01$.

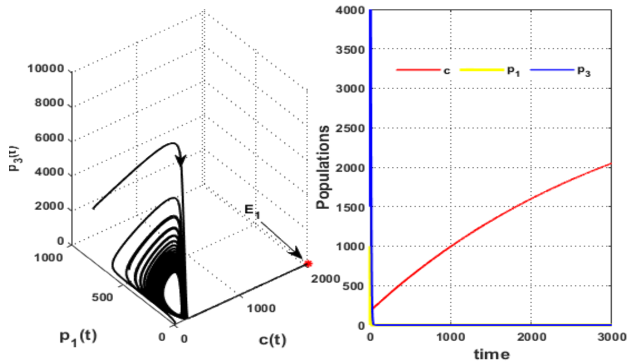

Figure 7. The existence and global stability for the parameters given in (21) with $e_2 = 0.001$.

For the data set (21) with a decrease in the human population decline rate coefficient attributable to CO_2 (e_7), the conditions (15-17) for the existence of a pair of purely imaginary roots of the characteristic eq 19 are satisfied, and the transversally condition is also satisfied under condition (18) when $e_7 \leq 0.00028$. The Hopf-bifurcation has occurred at $e_7^* = 0.00028$, as stated in Theorem 9. See Fig 8. Moreover, the same result could be obtained for the redaction of the human population expansion resulting from forest biomass(e_8). In this case, system (1) also faces a periodic attractor for $e_8 \leq 0.03$. See Fig 9.

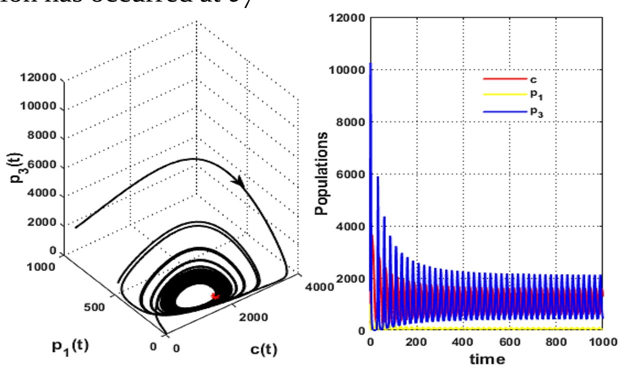

Figure 8. The existence of a periodic attractor for the dataset given in (21) with $e_7 = 0.00028$.

Published Online First: November, 2024
https://doi.org/10.21123/bsj.2024.11370
P-ISSN: 2078-8665 - E-ISSN: 2411-7986
Baghdad Science Journal

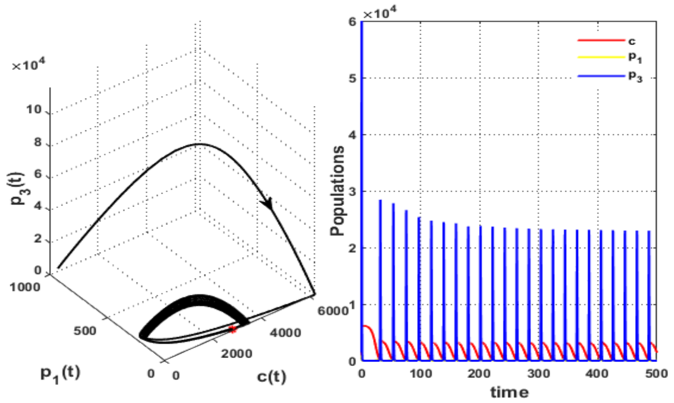

Figure 9. The existence of a periodic attractor for the dataset given in (21) with $e_8 = 0.03$.

- **The system with reforestation**

In this case, it is examined the interaction dynamics between all components in system (1). Upon analyzing the data set in (21), it observes that all prerequisites for the existence and global stability of $E_6 = (519, 167.67, 896.53, 1419.01)$ are met. See Fig 10.

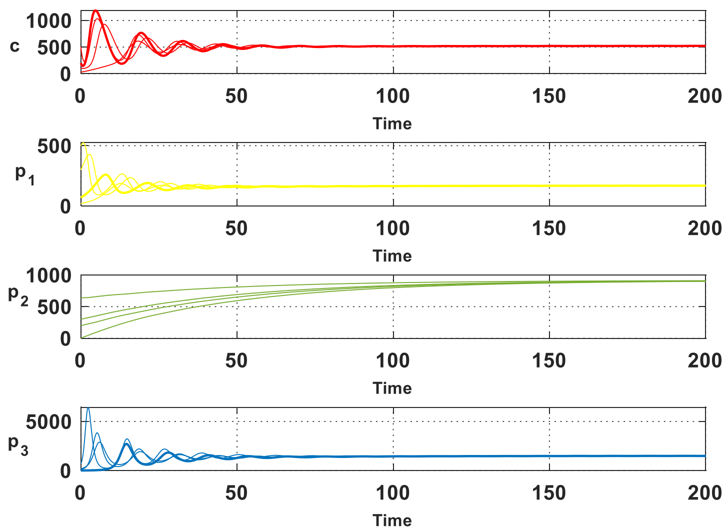

Figure 10. The existence and global stability of the parameters (21).

The impact of the coefficient of implementation rate for reforestation initiatives (r_3) is shown in Figs 11-12. Fig 11 shows for $r_3 \leq 0.00002$, the system faces loss in the reforestation effort, and the solution converges asymptotically to the reforestation-free equilibrium point $E_5 = (\ddot{c}, \ddot{p}_1, 0, \ddot{p}_3) = (469.58, 135.45, 0, 1063.26)$. While, for $0.00002 < r_3 < 0.28$, the system approaches the reforestation equilibrium point E_6. See Fig 10. While the system faces a periodic attractor for the range $r_3 \geq 0.28$. See Fig 12. So, the decrease in r_3 causes reforestation efforts have been rendered futile.

Published Online First: November, 2024
https://doi.org/10.21123/bsj.2024.11370
P-ISSN: 2078-8665 - E-ISSN: 2411-7986
Baghdad Science Journal

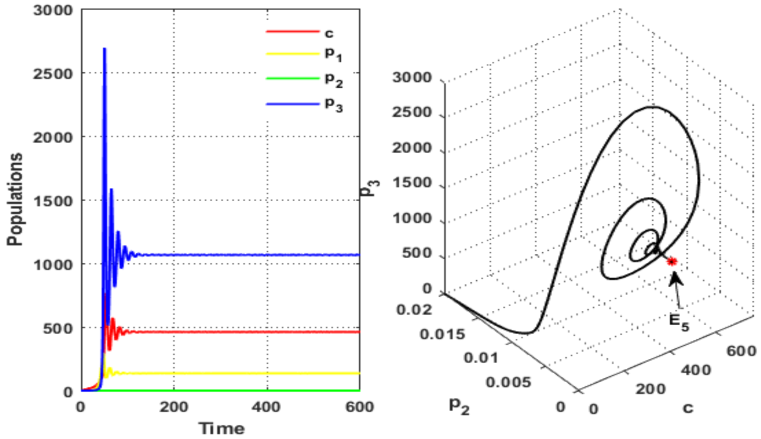

Figure 11. The solution of system (1) for the parameters given in (21) with $r_3 = 0.00002$.

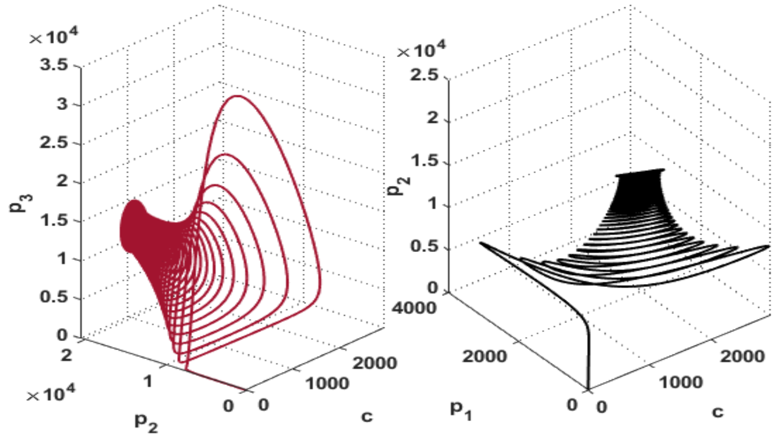

Figure 12. The face plane in cp_2p_3 space and cp_1p_2 space for the dataset given in (21) with $r_3 = 0.28$.

In addition, the conditions for stipulating the presence of two purely imaginary roots and satisfying the transversality condition fulfilled for the data set (21) with $e_8 \leq 0.02$. Therefore, the Hopf-bifurcation has occurred at $e_8^* = 0.02$, as stated in Theorem 10. See Fig 13.

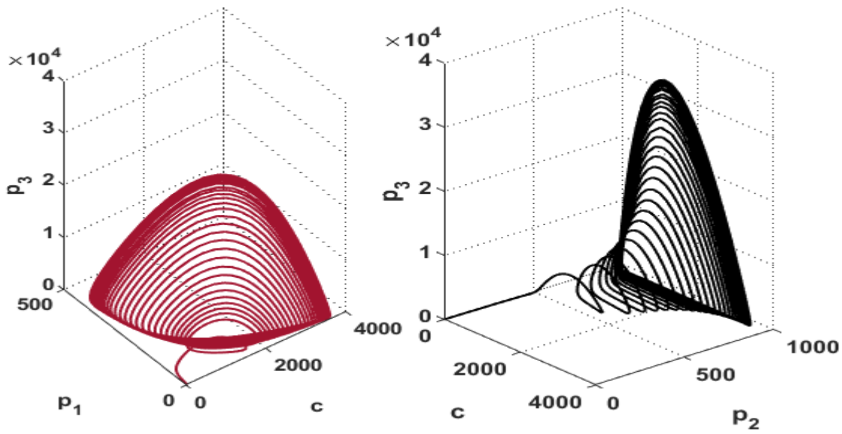

Figure 13. The Hopf bifurcation in cp_1p_3 space and cp_2p_3 space for the dataset given in (21) with $e_8^* = 0.02$.

Published Online First: November, 2024
https://doi.org/10.21123/bsj.2024.11370
P-ISSN: 2078-8665 - E-ISSN: 2411-7986
Baghdad Science Journal

The periodic attractor could also be obtained for the following cases $e_2 \leq 0.01$, $e_5 \geq 0.01$, $e_6 \leq 0.002$, and $e_7 \leq 0.0001$. See Figs 14-17.

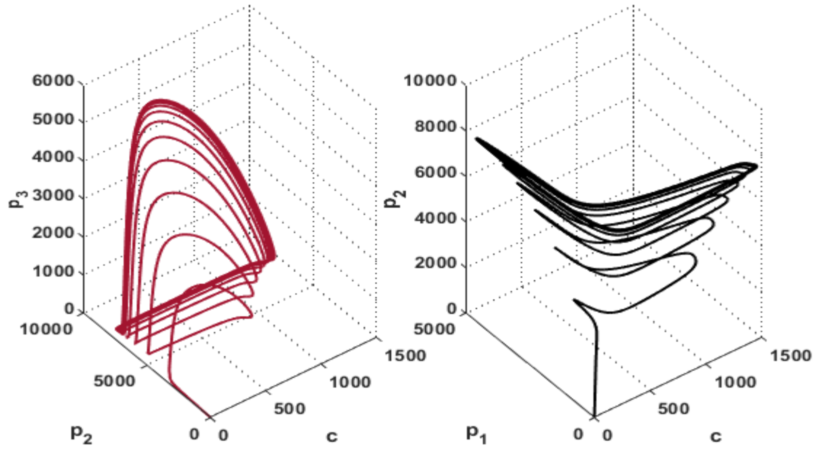

Figure 14. The periodic attractor in cp_2p_3 space and cp_1p_2 space for the dataset given in (21) with with $e_2 = 0.01$.

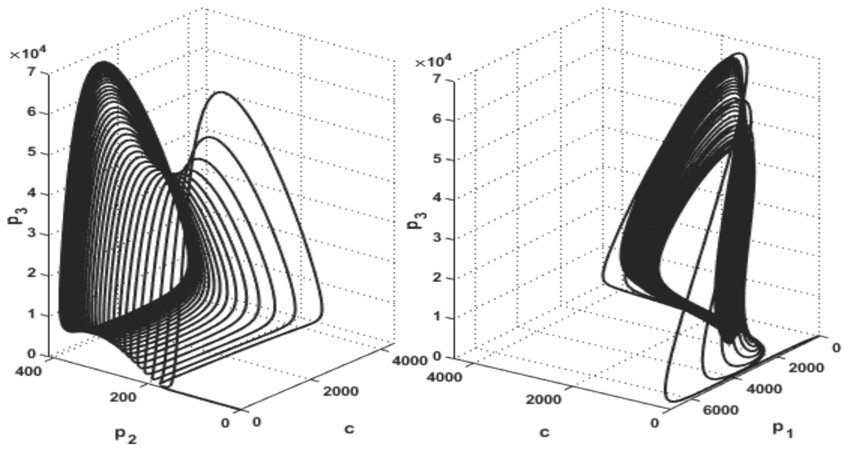

Figure 15. The periodic attractor in cp_2p_3 space and cp_1p_3 space for the dataset given in (21) with with $e_5 = 0.01$.

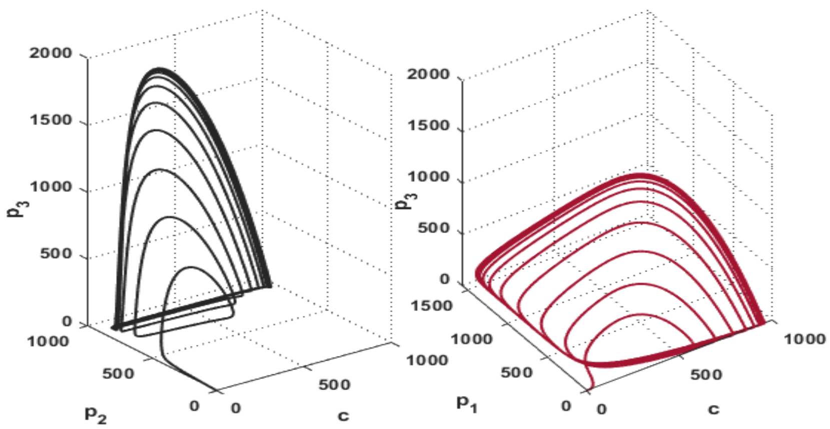

Figure 16. The periodic attractor in cp_2p_3 space and cp_1p_3 space for the dataset given in (21) with with $e_6 = 0.002$.

Published Online First: November, 2024
https://doi.org/10.21123/bsj.2024.11370
P-ISSN: 2078-8665 - E-ISSN: 2411-7986
Baghdad Science Journal

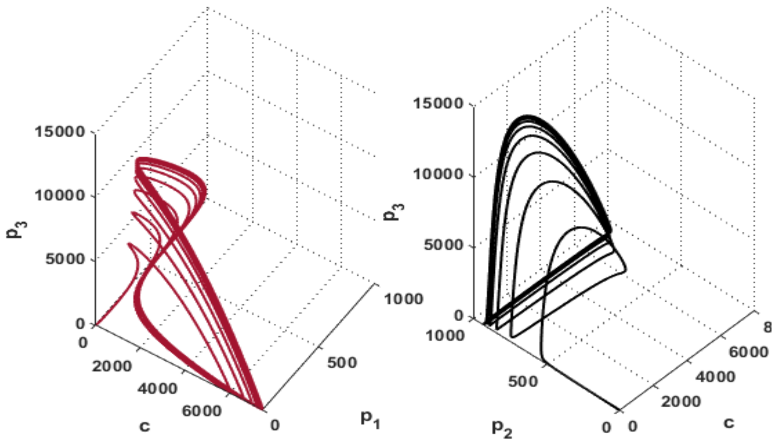

Figure 17. The periodic attractor in cp_1p_3 space and cp_2p_3 space for the dataset given in (21) with with $e_7 = 0.0001$.

Conclusion

This article suggests and analyses a nonlinear mathematical model to determine how low-density forest biomass and reforesting affect the flow of carbon dioxide into the atmosphere. To develop the model, it has been hypothesized that the concentration of carbon dioxide in the atmosphere rises due to both anthropogenic and natural activities, falls naturally, and absorbs carbon dioxide through forest biomass. It is also postulated that the increased mortality rate of the human population is a consequence of the detrimental impacts of carbon dioxide. Additionally, it is postulated that the human population consistently exploits forest biomass to sustain itself. As a result of population growth, forest areas are removed for agricultural and infrastructure development, which merely reduces the forest biomass's carrying capacity. The model under consideration comprises six non-negative equilibria. The conditions for both the feasibility and stability of these equilibria have been derived. The transcription and Hopf bifurcation around equilibria have been discussed. According to the model study, if reforestation is not implemented, certain elements would face the risk of extinction. Conversely, the concentration of CO_2 in the atmosphere would fall when reforestation was implemented. Furthermore, the analysis shows the system with reforestation has a stabilizing influence on the dynamics of the system. That means the system with reforestation has a stabilizing effect on the dynamics of the system. To guide our future work, a time delay in carrying out reforestation will be considered in the proposed system. Subsequently, the outcome will be juxtaposed with the findings presented in this research article.

Acknowledgment

The authors would like to thank this study's participants for their help and cooperation.

Authors' Declaration

- Conflicts of Interest: None.
- We hereby confirm that all the Figures and Tables in the manuscript are ours. Furthermore, any Figures and images, that are not ours, have been included with the necessary permission for re-publication, which is attached to the manuscript.
- No animal studies are present in the manuscript.
- No human studies are present in the manuscript.
- Ethical Clearance: The project was approved by the local ethical committee at University of Baghdad.

Authors' Contribution Statement

S.J. came up with the idea and oversaw its execution. F.N. analyzed its outcomes and penned its manuscript. M.W. and A.Z. read and approved the final manuscript. All authors had a hand in revising the final paper and discussing the findings

References

1. Brown S. Tropical forests and the global carbon cycle: the need for sustainable land-use patterns. Agric Ecosyst Environ. 1993; 46(1–4): 31–44. https://doi.org/10.1016/0167-8809(93)90011-D
2. Thirthar AA, Sk N, Mondal B, Alqudah MA, Abdeljawad T. Correction: Utilizing memory effects to enhance resilience in disease-driven prey-predator systems under the influence of global warming. J Appl Math Comput. 2023; 69: 4909–4910. https://doi.org/10.1007/s12190-023-01963-8
3. Thirthar AA, Panja P, Khan A, Alqudah MA. An Ecosystem Model with Memory Effect Considering Global Warming Phenomena and Exponential Fear Function. Fractals. 2023; 31(10): 1–19. https://doi/10.1142/S0218348X2340162X
4. Makarov I, Chen H, Paltsev S. Impacts of climate change policies worldwide on the Russian economy. Clim Policy. 2020 Nov 25; 20(10): 1242-56. https://doi.org/10.1080/14693062.2020.1781047
5. Dubey B, Sharma S, Sinha P, Shukla JB. Modelling the depletion of forestry resources by population and population pressure augmented industrialization. Appl Math Model. 2009; 33(7): 3002–3014. https://doi.org/10.1016/j.apm.2008.10.028
6. Panja P. Is the forest biomass a key regulator of global warming?: A mathematical modelling study. Geol Ecol Landsc. 2022 Jan 2; 6(1): 66-74. https://doi.org/10.1080/24749508.2020.1752021.
7. Panja P. Deforestation, Carbon dioxide increase in the atmosphere and global warming: A modelling study. Int J Model Simul. 2021 May 4; 41(3): 209-219. https://doi.org/10.1080/02286203.2019.1707501.
8. Caetano MAL, Gherardi DFM, Yoneyama T. An optimized policy for the reduction of CO2 emission in the Brazilian Legal Amazon. Ecol Model. 2011; 222(15): 2835–2840. https://doi.org/10.1016/j.ecolmodel.2011.05.003
9. Janssens-Maenhout G, Crippa M, Guizzardi D, Muntean M, Schaaf E, Dentener F, et al. EDGAR v4. 3.2 Global Atlas of the three major greenhouse gas emissions for the period 1970–2012. Earth Syst Sci Data. 2019 Jul 8; 11(3):959-1002. https://doi.org/10.5194/essd-11-959-2019
10. Morales-Hidalgo D, Oswalt SN, Somanathan E. Status and trends in global primary forest, protected areas, and areas designated for conservation of biodiversity from the Global Forest Resources Assessment 2015. For Ecol Manag. 2015; 352: 68–77. https://doi.org/10.1016/j.foreco.2015.06.011
11. Van Wees D, van Der Werf GR, Randerson JT, Andela N, Chen Y, Morton DC. The role of fire in global forest loss dynamics. Glob Change Biol. 2021 Jun; 27(11): 2377-2391. https://doi.org/10.1111/gcb.15591
12. Shukla JB, Dubey B. Modelling the depletion and conservation of forestry resources: effects of population and pollution. J Math Biol. 1997; 36(1): 71–94. https://doi.org/10.1007/s002850050091
13. Tennakone K. Stability of the biomass-carbon dioxide equilibrium in the atmosphere: mathematical model. Appl Math Comput. 1990; 35(2): 125–130. https://doi.org/10.1016/0096-3003(90)90113-H
14. Shukla JB, Chauhan MS, Sundar S, Naresh R. Removal of carbon dioxide from the atmosphere to reduce global warming: a modelling study. Int J Glob Warm. 2015; 7(2): 270–292. https://doi.org/10.1504/IJGW.2015.067754
15. Kim YW, Kim T, Shin J, Go B, Lee M, Lee J, et al. Forecasting Abrupt Depletion of Dissolved Oxygen in Urban Streams Using Discontinuously Measured Hourly Time-Series Data. Water Resour Res. 2021 Apr; 57(4): 1-14. https://doi.org/10.1029/2020WR029188
16. Misra AK, Verma M. Impact of environmental education on mitigation of carbon dioxide emissions: a modelling study. Int J Glob Warm. 2015; 7(4): 466–486. https://doi.org/10.1504/IJGW.2015.070046
17. Misra AK, Chandra P, Raghavendra V. Modeling the depletion of dissolved oxygen in a lake due to algal bloom: Effect of time delay. Adv Water Resour. 2011; 34(10): 1232–1238. https://doi.org/10.1016/j.advwatres.2011.05.010
18. Misra AK, Verma M, Venturino E. Modeling the control of atmospheric carbon dioxide through reforestation: effect of time delay. Model Earth Syst Environ. 2015; 1(3): 1-17. https://doi.org/10.1007/s40808-015-0028-z
19. Altamirano-Fernández A, Rojas-Palma A, Espinoza-Meza S. Optimal Management Strategies to Maximize Carbon Capture in Forest Plantations: A Case Study

with Pinus radiata D. Don. Forests. 2023; 14(1): 1-17. https://doi.org/10.3390/f14010082
20. Bulatkin GA. A New Model for Calculating the Impact of Forests and Wood Use on the Balance of C-CO_2 in the Earth's Atmosphere. Proceedings of the 3rd International Electronic Conference on Forests—Exploring New Discoveries and New Directions in Forests. Environ Sci Proc. 2022; 22(1): 1-7. https://doi.org/10.3390/IECF2022-13040
21. Mostafaeipour A, Bidokhti A, Fakhrzad MB, Sadegheih A, Mehrjerdi YZ. A new model for the use of renewable electricity to reduce carbon dioxide emissions. Energy. 2022 Jan 1; 238(Part A): 121602. https://doi.org/10.1016/j.energy.2021.121602
22. Morris DW. Measuring the Allee Effect: Positive Density Dependence in Small Mammals. Ecology. 2002; 83(1): 14–20. https://doi.org/10.1890/0012-9658(2002)083[0014:MTAEPD]2.0.CO;2
23. Chen B. Dynamic behaviors of a commensal symbiosis model involving Allee effect and one party can not survive independently. Adv Differ Equ. 2018; 2018(1): 1–12. https://doi.org/10.1186/s13662-018-1663-2
24. Dennis B. Allee Effects: Population growth, Critical density, and the Chance of Extinction. Nat Resour Model. 1989; 3(4): 481–538. https://doi.org/10.1111/j.1939-7445.1989.tb00119.x
25. Kuznetsov N, Reitmann V. Attractor Dimension Estimates for Dynamical Systems: Theory and Computation. Switzerland: Springer; 2020. 545 p. https://doi.org/10.1007/978-3-030-50987-3
26. LaSalle JP. Stability Theory and Invariance Principles. In: Cesari L, Hale JK, LaSalle JP, editors. Dynamical systems. Academic Press; 1976. p. 211–222. https://doi.org/10.1016/B978-0-12-164901-2.50021-0
27. Meng X-Y, Xiao L. Stability and Bifurcation for a Delayed Diffusive Two-Zooplankton One-Phytoplankton Model with Two Different Functions. Complexity. 2021; 2021(1): 1-24. https://doi.org/10.1155/2021/5560157
28. Zeb A, Zaman G, Momani S. Square-root dynamics of a giving up smoking model, Applied Mathematical Modelling 37 (7), 5326-5334. https://doi.org/10.1016/j.apm.2012.10.005.
29. Collings JB. Bifurcation and stability analysis of a temperature-dependent mite predator-prey interaction model incorporating a prey refuge. Bull Math Biol. 1995; 57(1): 63–76. https://doi.org/10.1007/BF02458316
30. Jawad S, Hassan SK. Bifurcation analysis of commensalism intraction and harvisting on food chain model. Braz J Biom. 2023; 41(3): 218–233. https://doi.org/10.28951/bjb.v41i3.609
31. Thirthar AA, Abboubakar H, Khan A, Abdeljawad T. Mathematical modeling of the COVID-19 epidemic with fear impact. AIMS Math. 2023; 8(3): 6447–6465. http://doi.org/2010.3934/math.2023326
32. Yousef A, Thirthar AA, Alaoui AL, Panja P, Abdeljawad T. The hunting cooperation of a predator under two prey's competition and fear-effect in the prey-predator fractional-order model. AIMS Math. 2022; 7(4): 5463–5479. https://doi.org/10.3934/math.2022303
33. Al-Jaf DS. The Role of Linear Type of Harvesting on Two Competitive Species Interaction. Commun Math Biol Neurosci. 2024; 2024: 1-25. https://doi.org/10.28919/cmbn/8426
34. Thirthar AA. A Mathematical Modelling of a Plant-Herbivore Community with Additional Effects of Food on the Environment. Iraqi J Sci. 2023; 64(7): 3551–3566. https://doi.org/10.24996/ijs.2023.64.7.34
35. Kareem AM, Al-Azzawi SN. Comparison between Deterministic and Stochastic Model for Interaction (COVID-19) With Host Cells in Humans. Baghdad Sci J. 2022 Oct 23; 19(5): 1140-1147. https://doi.org/10.21123/bsj.2022.6111.
36. Hameed HH, Al-Saedi HM. Three-Dimensional Nonlinear Integral Operator with the Modelling of Majorant Function. Baghdad Sci J. 2021 Jun 1; 18(2): 296-305. http://dx.doi.org/10.21123/bsj.2021.18.2.0296.
37. Ali A, Jawad S. Stability analysis of the depletion of dissolved oxygen for the Phytoplankton-Zooplankton model in an aquatic environment. Iraqi J Sci. 2024 May 30; 65(5): 2736-2748. https://doi.org/10.24996/ijs.2024.65.5.31.
38. Haque M, Venturino E. Increase of the prey may decrease the healthy predator population in presence of a disease in the predator. HERMIS. 2006; 7: 38-59.

Published Online First: November, 2024
https://doi.org/10.21123/bsj.2024.11370
P-ISSN: 2078-8665 - E-ISSN: 2411-7986
Baghdad Science Journal

تحليل الاستقرارية لنموذج الانبعاث المفرط لثاني أكسيد الكربون من خلال اتباع سياسة إعادة التشجير في الغابات منخفضة الكثافة

فرقان نزار[1]، شيرين جواد[1]، ماثياس ونتر[2]، انور زاب[3]

[1]قسم الرياضيات ياضيات، كلية العلوم، جامعة بغداد، بغداد، العراق.
[2]قسم الرياضيات، جامعة برونيل لندن، اوكسبردج، المملكة المتحدة.
[3]قسم الرياضيات، جامعة كومساتس إسلام آباد، حرم أبوت آباد، باكستان.

الخلاصة

يعتبر غاز ثاني أوكسيد الكاربون مسبب رئيسي لظاهرة الاحتباس الحراري. تعتبر الكتلة الحيوية للغابات ضرورية لاحتجاز ثاني أوكسيد الكاربون في الغلاف الجوي؛ ومع ذلك، فإن معدل الانخفاض في الكتلة الحيوية للغابات في جميع أنحاء العالم مثير للقلق ويمكن أن يعزى إلى الأنشطة البشرية. تعد إعادة التشجير أمرًا ضروريًا في هذه الحالة لتقليل كمية ثاني أوكسيد الكاربون في الغلاف الجوي. يمكن تقييم جهود إعادة التشجير وفقًا للاستثمار المالي المطلوب لتنفيذها. يقدم هذا العمل نموذجًا رياضيًا غير خطي يدرس تأثير إعادة التشجير وتنفيذ مبادرات إعادة التشجير على تنظيم مستويات غاز ثاني أوكسيد الكاربون في الغلاف الجوي. تم العثور على القيم الحرجة للنموذج وتم تحليل استقرارها . تم إجراء تحليل التشعب حول القيم الحرجة المحتملة. واستنادا إلى تحليل النموذج، فإن غياب إعادة التشجير من شأنه أن يعرض بعض الجوانب لخطر الانقراض. في حين ساهم برنامج اعادة التشجير في انخفاض مستوى ثاني أوكسيد الكاربون في الغلاف الجوي. علاوة على ذلك، يشير التحليل الرقمي إلى أن النظام يعاني من فقدان الاستقرار دون أنشطة إعادة التشجير.في حين يحافظ النظام على التذبذب من خلال تشعب هوبف أثناء الانخراط في أنشطة إعادة التشجير.

الكلمات المفتاحية: تحليل التشعب، نموذج غاز ثاني اوكسيد الكاربون، تحليل عددي، اعادة التشجير، تحليل الاستقرارية.